iEnergy

REVIEW

https://doi.org/10.23919/IEN.2023.0001

Eco-friendly gas insulating medium for next-generation SF_6-free equipment

Yi Li[1,2], Shuangshuang Tian[1], Linlin Zhong[3], Geng Chen[4], Song Xiao[2], Yann Cressault[5], Yuwei Fu[6], Yu Zheng[2], Christophe Preve[7], Zhaolun Cui[8], Yin Zhang[1], Fanchao Ye[1], Daniel Piccoz[7], Gang Wang[7], Yalong Li[1], Youping Tu[4], Wenjun Zhou[2], Ju Tang[2] and Xiaoxing Zhang[1] ✉

ABSTRACT

Gas-insulated equipment (GIE) that utilizes the most potent greenhouse gas sulfur hexafluoride (SF_6) as insulation and arc-quenching medium has been widely used in the power industry. Seeking eco-friendly insulating gas with advanced performance for next-generation SF_6-free GIE is significant for the “net-zero” goal and sustainable development. In this paper, the utilization, emission, and reduction policies of SF_6 around the world were summarized first. Then, we systematically reviewed the latest progress in comprehensive performance evaluation of eco-friendly insulating gas in terms of molecular design, dielectric insulation, arc-quenching, stability and decomposition, materials compatibility, biosafety, etc. Further, the representative applications of eco-friendly insulating gas in medium-voltage, high-voltage GIE as well as relevant maintenance-related technologies were highlighted. Accordingly, the existing challenges and future perspectives were proposed, presenting a roadmap to hopefully steer the development of eco-friendly insulating gas and GIE.

KEYWORDS

Eco-friendly insulating gas, net-zero, dielectric insulation, arc-quenching, SF_6-free gas-insulated equipment (GIE).

Gas-insulated equipment (GIE) including gas-insulated switchgear (GIS), gas-insulated transmission line (GIL), gas-insulated transformer (GIT), gas-insulated cabinet (GIC) with the advantages of small footprint, high reliability, long maintenance cycle has been widely used in the power system of various voltage levels[1,2]. Normally, sulfur hexafluoride (SF_6) is utilized as the insulation and arc-quenching medium for GIE owing to its superior dielectric performance. However, SF_6 is one of the most potent greenhouse gases with a global warming potential (GWP) of 25,200 and an atmospheric lifetime of 3,200 years[3,4]. The power industry accounts for 80% of the SF_6 consumption, which value reaches over 7,000 tons in China[5,6]. Moreover, the global SF_6 emission amount demonstrates an increasing trend at the rate of 10% annually, whose atmospheric content changes from 3.67 part per trillion (ppt) in 1994 to 10.41 ppt in 2020[7,8]. The design and application of eco-friendly insulating gas to substitute SF_6 for next-generation GIE are necessary and urgent currently to achieve the “carbon peak, carbon neutral” and “net-zero” emission[9].

Up to now, various gases have been focused as potential substitutes to SF_6 owing to their low GWP and superior dielectric strength, such as perfluorocarbons (PFCs), trifluoroiodomethane, fluorinated nitrile, fluorinated ketones, hydrofluro-olefins (HFOs), etc. The assessment of the application feasibility of the proposed eco-friendly gas is also conducted to provide basic information for GIE design and engineering application. Meanwhile, various theoretical analysis technologies have been relatively mature in exploring the micro-mechanism of gas insulation, leading to performance prediction and molecular design. Further, some pioneering eco-friendly insulating gas-based equipment has been developed for engineering applications. Relevant progress has also been summarized. Specifically, Rabie et al. and Franck et al. provided an overview of gas insulation, the climate impact of SF_6 and development of eco-friendly insulating gas for SF_6-free medium-voltage (MV) and high-voltage (HV) GIE[10,11]. The advances in the quest for eco-friendly insulating gas were reviewed by Beroual et al.[12] Further, Li et al. and Zhang et al. summarized the fundamental physicochemical properties of eco-friendly insulating gas for GIS application, where the basic data calculations and fundamental experiments for performance evaluation were emphasized[13,14]. The stability and decomposition characteristics were reviewed by Xiao et al. and Yang et al, which guides the reliable application of eco-friendly insulating gas[15,16]. The in-detail characteristics of C_4F_7N, $C_5F_{10}O$ were also summarized by Pan et al. and Owens et al.[17,18] Challenges primarily remained on the problems such as inferior stability, weaker arc extinguishing performance, hazardous by-product generation, etc. The feasibility of eco-friendly insulating gas for GIL application was also evaluated by Tu et al.[19,20]

Herein, we highlight recent advances in eco-friendly insulating gas for next-generation SF_6-free GIE. Firstly, we provide an

[1]Hubei Engineering Research Center for Safety Monitoring of New Energy and Power Grid Equipment, Hubei University of Technology, Wuhan 430068, China; [2]School of Electrical Engineering and Automation, Wuhan University, Wuhan 430072, China; [3]School of Electrical Engineering, Southeast University, Nanjing 210096, China; [4]State Key Laboratory of Alternate Electric Power System with Renewable Energy Sources, North China Electric Power University, Beijing 102206, China; [5]LAPLACE (Laboratoire Plasma et Conversion d'Energie), Université de Toulouse, Toulouse 31013, France; [6]Department of Electrical Engineering, Xi’an University of Technology, Xi’an 710048, China; [7]Schneider Electric, Reuil-Malmaison 92500, France; [8]School of Electric Power Engineering, South China University of Technology, Guangzhou 510006, China

Address correspondence to Xiaoxing Zhang, xiaoxing.zhang@outlook.com

overview of the SF_6-based GIE, followed by the emission and reduction policies of SF_6 to clarify the necessity of seeking eco-friendly insulating gas. Secondly, the basic requirements, categories and molecular design of eco-friendly insulating gas are summarized, indicating the main performance assessment dimensions. Thirdly, we highlight recent progress of various eco-friendly insulating gas in terms of molecular design, dielectric insulation, arc-quenching, stability and decomposition, materials compatibility, biosafety. After that, we summarized the latest application of eco-friendly insulating gas in MV, HV scenarios as well as relevant maintenance-related technologies. Finally, we discuss the existing challenges and propose perspectives for future research. We believe this review could provide insights into the development of eco-friendly gas insulating medium as well as next-generation SF_6-free GIE.

1 Utilization and emission of SF_6

1.1 SF_6-based GIE

SF_6 is successfully synthesized by Moissan and Lebeau in 1900 and applied as dielectric insulation and arc-quenching medium since the 1960s[12]. Pure SF_6 is non-toxic, non-flammable, noncorrosive and physiochemical stable, which is suitable for various application fields including the power industry, mining engineering, semiconductor processing, optical engineering and health care[21]. GIE for electricity transmission and distribution accounts for 80% of SF_6 consumption, followed by magnesium casting and aluminum smelting (as shown in Figure 1(a)). Specifically, the annual SF_6 utilization in China demonstrates an increasing trend (Figure 1(b)), which changes from 3,200 tons (2008) to 7,000 tons (2018).

SF_6 possesses superb dielectric strength that is about three times of air at atmospheric pressure (0.1 MPa) and similar to that of transformer oil at 0.3 MPa, which is ascribed to its strong free electrons capture ability, forming heavy ions and preventing the formation of electron flow (Figure 1(c)). Besides, SF_6 has high heat capacity and low viscosity, which is an excellent gas for arc-quenching. Specifically, SF_6 is capable of absorbing arc energy and remaining conductive at low temperatures, which minimizes current chopping and avoids overvoltage[22–24]. The arc-quenching capability of SF_6 reaches ~10 times that of air. More importantly, the decomposed particles (SF_x) could recombine to SF_6 after a high energy arc, making it suitable for repeated current interruption (Figure 1(d))[22]. The world's first SF_6 GIS was developed and applied in the United States (US) in 1950s[25]. Then the use of SF_6-based GIE became widespread in the late 1960s in Europe. In 1971, the first 110 kV fully SF_6 insulated GIS and 35 kV circuit breaker (CB) was independently developed in China. Since then, SF_6 plays a dominant role in high voltage, ultrahigh voltage (UHV), and extra-high voltage (EHV) GIE for electricity transmission[26].

1.2 SF_6 emission

As introduced in previous section, the emission of SF_6 demonstrates a fast increasing trend, especially in developing countries. According to the report of Simmonds et al.[27], the global emission rate of SF_6 is 7.3 ± 0.6 $Gg{\cdot}yr^{-1}$ (1 Gg=1000 t) in 2008 and it shows an increase of 24% to 9.04±0.35 $Gg{\cdot}yr^{-1}$ in 2018, as shown in Figure 2(a). The maintenance, replacement, and continuous leakage of the GIE are the main reasons for new additional emissions. Accordingly, the SF_6 loading of the atmosphere has increased by a factor of about 15 from 1978 to 2018, achieving a global radiative forcing of 5.5± 0.1 $mW{\cdot}m^{-2}$ to the total environment[28]. Among all the countries, China shows the largest emission scale with a rapid increase since the beginning of this century (Figure 2(b)). The global installed electrical capacity can be found in Figure 2(c). In 2018, the installed electrical capacity reached 1,899.7 GW, resulting in an estimated emission of SF_6 to be 5.19 Gg, which accounts for about 75.9% of the total SF_6 emission from the electrical aspects[27]. It should be noted that China has the largest electrical loading since 2015, corresponding to an annual emission of SF_6 of 3,500 tons

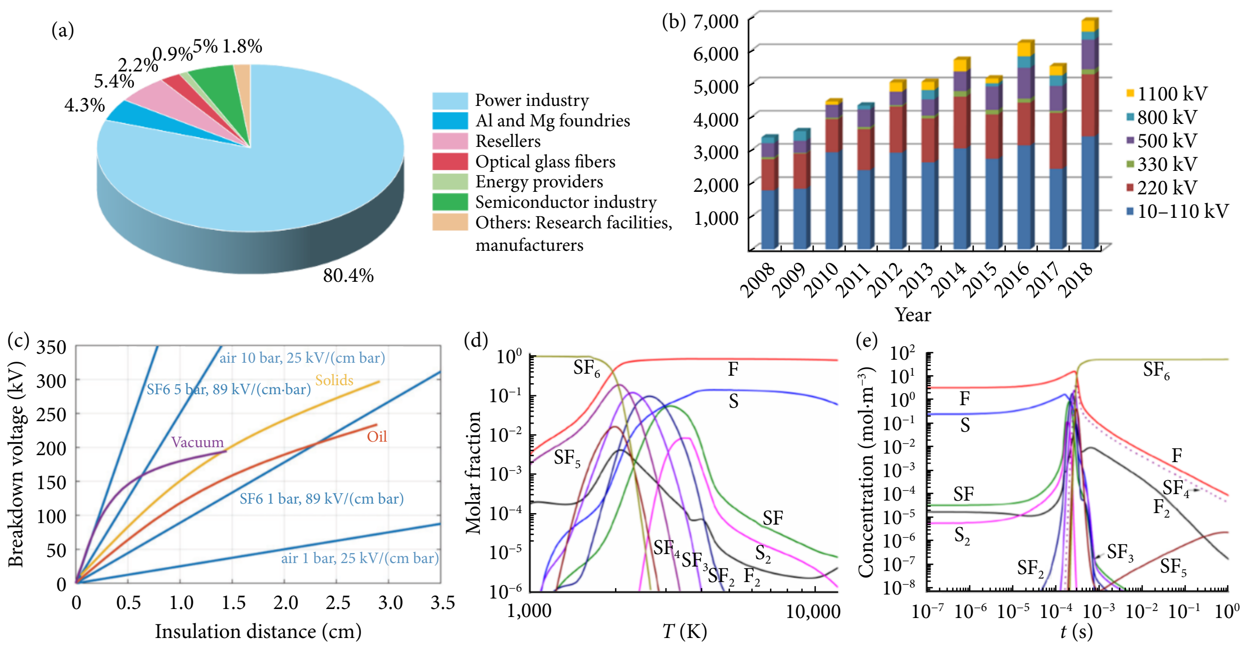

Fig. 1 The properties and application of SF_6. (a) The application of SF_6 in various fields. Source: Federal Statistical Office: Survey of particular climate-active materials "sulfur hexafluoride" (SF_6), Wiesbaden, 2015. **(b)** The annual SF_6 utilization in China for GIS. Source: Report on alternative technologies of sulfur hexafluoride in the power industry. **(c)** The dielectric insulation performance of SF_6 compared with oil, solids and air. Reprinted with permission from Ref. [11], © 2021 IEEE. **(d,e)** The molar fraction of neutral particles versus temperature and time in the SF_6 arc plasma. Reprinted with permission from Ref. [22], © 2016 IOP Publishing Ltd.

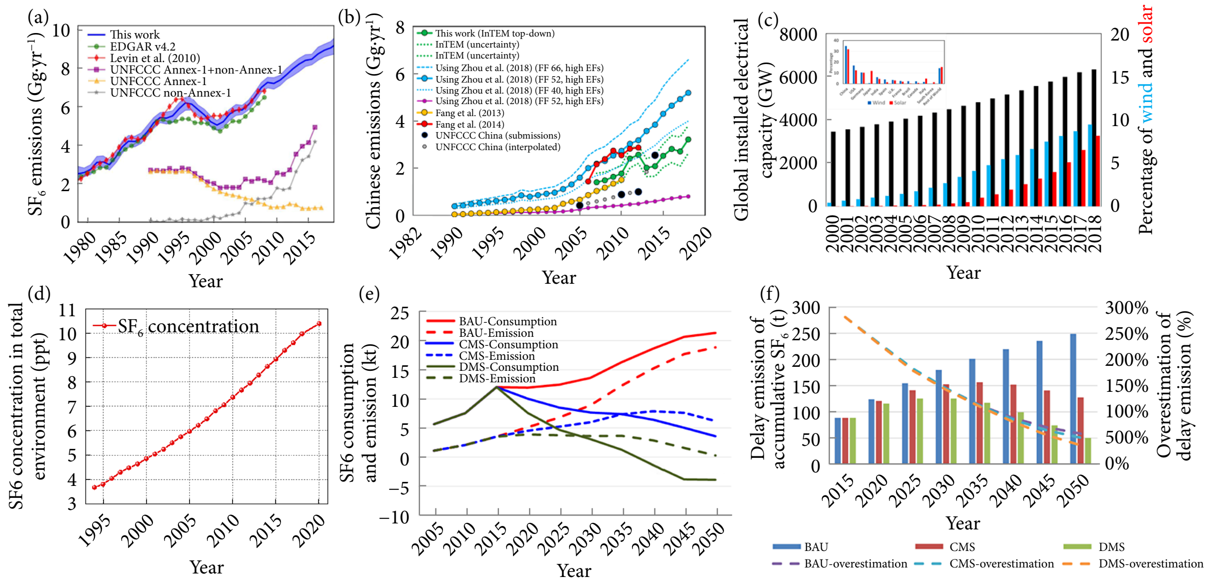

Fig. 2 Emission statistics of SF_6. (a) Total emission of SF_6 around the world from 1980 to 2015. Reprinted with permission from Ref. [27], © 2020 Author(s). **(b)** Estimated emission of SF_6 in China from 1990. Reprinted with permission from Ref. [27], © 2020 Author(s). (c) Global installed electrical capacity (GW). Reprinted with permission from Ref. [27], © 2020 Author(s). **(d)** Variation of SF_6 concentration in the total environment since 1994. Source: Global Monitoring Laboratory, Earth System Research Laboratories[7]. **(e)** Predictions of SF_6 consumption (solid lines) and emission (dotted lines) (kt) in China under three estimation methods. Reprinted with permission from Ref. [8], © 2018 Author(s). **(f)** Prediction of the SF_6 delayed emission effect to 2050. Reprinted with permission from Ref. [8], © 2018 Author(s).

this year[8]. According to the International Energy Organization, global electricity demand is expected to grow by 30% between 2015 and 2040, and is mainly concentrated in developing countries, which lays a great demand for the development of mature eco-friendly insulation equipment[8].

By contrast, the SF_6 emission in the US and EU countries are relatively reduced in recent decades. As introduced by the US Environmental Protection Agency (USEPA), the SF_6 emission in the USA in 2020 was about 0.236,8 Gg (~5,967.36 Gg CO_2e)[29]. The European Environment Agency has 0.028,6 tons (~720 Gg CO_2e) SF_6 emission of EU in 2017. The lower emission is attributed to the smaller electrical loadings, more complete SF_6 full-cycle management and already-applied eco-friendly insulation equipment compared to China[30].

The SF_6 atmospheric concentration increased rapidly from ~3.6 ppt (part per trillion) in 1994 to 10.3 ppt in 2020, as shown in Figure 2(d). Moreover, a so-called "delayed emission effect" might happen in China and other countries, leading to a sharp increase in SF_6 emissions (Figure 2(e))[8]. It's attributed to the potential retirement of GIE in the following decades, and the cumulative delayed emission is expected to be 50~249 kt, corresponding to 1.2~6.0 Gt CO_2e (Figure 2(f)). In this case, the development of eco-friendly insulating gases is also time-critical.

1.3 SF_6 reduction policies

SF_6 was labeled as the most potent greenhouse gas in 1995 by the Inter-governmental Panel on Climate Change (IPCC). In 1997, the Kyoto protocol identified SF_6 as the six types of the most greenhouse gases that need to be severely restricted[31]. Frankly, the climate concern of SF_6 attributes to its stable molecular structure that endures an extremely atmospheric lifetime. The proficient absorption of infrared radiation further leads to the high GWP of SF_6. In 2009, the US identified SF_6 as "a threat to the health and welfare of current and future generations due to their effects on world climate" under section 202(a) of the Clean Air Act[32]. The European Union Regulation No. 842-2006 and No. 517/2014. established the rules on the use, recovery and treatment of fluoride gases including SF_6, which also requires that the emission of SF_6 should be less than 0.1% and the assessment of SF_6 replacements in new MV no later than 2020[33,34]. Europe is committed to net zero emission of carbon by 2050. Fluorinated gases used for air conditioning, heat pump, switchgear are participating significantly to carbon emissions. That is why European Commission has decided to propose further improvements to the current F-gases regulation. The draft has been issued in April 2022 and is in discussion for amendments in environmental and industry committees of the European parliament, and country representatives. The vote on the final document by European parliament should happen before the end of 2023. Specifically, the draft proposes to ban gases with GWP > 10 for HV and MV switchgear. However, in order to ensure the continuity of switchgear market, derogation will be given if no solution with gas GWP < 10 is available on the market. In that case, gas with GWP < 2,000 will be accepted. If no solution with GWP gas < 2,000 is available, SF_6 can be accepted. An open tender should be made for switchgear and in case of non-availability of gas GWP < 10, results should be documented for future verification. Table 1 indicates dates of F-gas GWP > 10 prohibitions according to voltage. Besides, the power grid company in Germany, Britain, and Republic of Korea also proposed to utilize SF_6-free GIE in 2030~2050.

The rapid growth of HV, UHV, EHV projects in China prompts the annual increase of SF_6 usage. In 2012, the GB/T

Table 1 Prohibition of F-gas GWP > 10 by European Commission.

Voltage level	Deadline
⩽ 24 kV	1st January 2026
⩽ 52 kV	1st January 2030
⩽ 145 kV, 50 kA	1st January 2028
>145 kV, 50 kA	1st January 2031

28537-2012 entitled the use and handling of SF6 in high-voltage switchgear and controlgear regulated the treatment during GIE installation, operation, maintenance and end of service[35]. Further, the GB/T-32151.2-2015 (Requirements of the greenhouse gas emissions accounting and reporting. Part 2: Power grid enterprise) stipulated the emission accounting of SF_6[36]. The State Grid and China Southern Power Grid also formulated relevant SF_6 life-cycle management and control policies, including the establishment of the recycling center, purification and reuse, etc. The SF_6/N_2 gas mixture based GIE has been put into operation since 2022. The increasingly severe policies and environmental status drive the design and application of eco-friendly insulating gas for next-generation SF_6-free GIE.

2 Development of eco-friendly insulating gas

2.1 Basic requirements for eco-friendly gas

Insulating gas undertakes the mission of electrical insulation and current interruption, which is the core component of GIE. The gas performance essentially determines the operation reliability, service life and maintenance cost of the equipment. The following requirements and selection criteria should be considered for the design or selection of SF_6 substitute gas, as heightened in Figure 3(a).

Environmental features

The low GWP, no ozone depleting potential (ODP), short atmospheric lifetime and low and are the basic requirements for eco-friendly insulating gas. Specifically, the GWP is related to the absorb ability of infrared rays, the wavelength range of the absorption spectrum and the atmospheric lifetime[37,38]. The ODP reflects the potential impact of substance gas escaping into the atmosphere on ozone destruction, which is mainly ascribed to the chlorine, bromine element and nitric oxide[39,40]. Besides, low liquefaction temperature is highly desired as it determines the minimum operating temperature of GIE (usually at −15~25°C).

Insulation & Arc-quenching

High electric strength and superior arc-quenching are the most significant properties of eco-friendly insulating gas. For dielectric insulation, the gas is expected to prevent the formation of electron avalanches or streamers up to high electric field stress[21]. The high ionization energy, low electron affinity of the gas molecule is desired to suppress the impact ionization and promotes electron attachment, detachment process that determines the critical electric field. For arc-quenching, the high current interruption capacity, superior heat dissipation and self-recovery performance should be considered. Importantly, the self-recovery ability of gas molecules after arc plasma decomposition determines the repeated quenching property and service life.

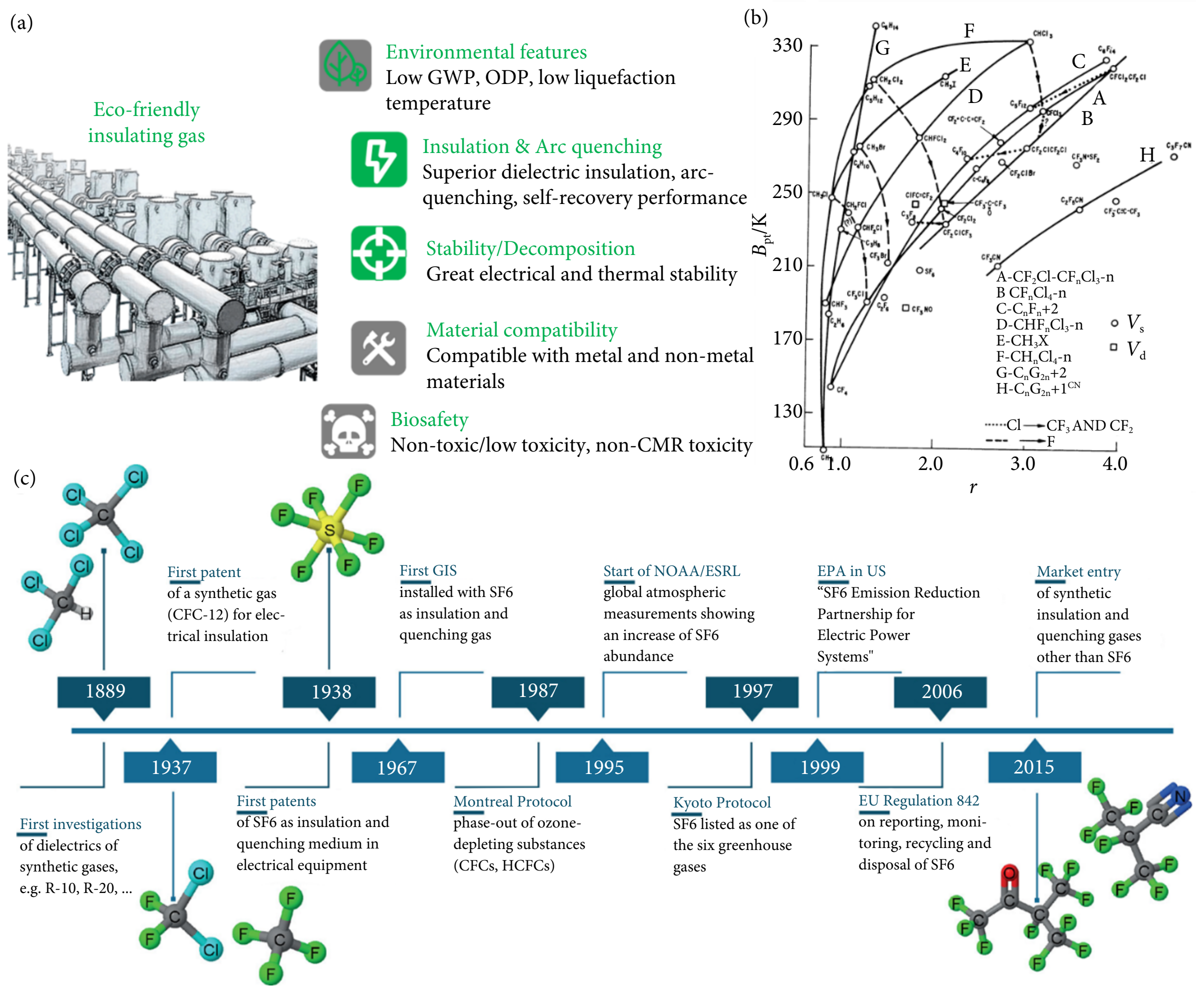

Fig. 3 The basic requirements and classification of eco-friendly insulating gas. (a) The five main properties of advanced insulating gas. **(b)** The relationship between dielectric strength relative to N_2 and boiling point. Reprinted with permission from Ref. [9], © 1980 IEEE. **(c)** The timeline regarding substances used for electrical insulation and crucial events concerning the use and development of insulation gases. Reprinted with permission from Ref. [10], © 2018 American Chemical Society.

Stability/Decomposition

The ideal insulating gas should have excellent thermal, electrical stability. Generally, various early latent defects will inevitably be introduced into the GIE due to transportation, installation, maintenance[41,42]. In addition, early insulation faults such as partial discharge (PD) or partial overheating fault (POF) may also occur under long-term operation, which will lead to the decomposition of gas molecules and generate various by-products. The thermal and discharge stability/decomposition condition, by-product type, content as well as the influence of various parameters (gas pressure, mixing ratio, impurities, etc.) should be addressed.

Material compatibility

Normally, GIE has a relatively long maintenance period (half a year) and decades of service life. More than one hundred different materials are used in GIE, which mainly can be classified into metals and alloys, insulators (epoxy resin), thermoplastics and thermosets, elastomer and adsorbent (desiccant)[43]. The high-pressure insulating gas may interact with various materials, inducing gas decomposition and material corrosion owing to the gas-solid thermal/electrical reactions. Investigations on the material's compatibility are necessary to evaluate the stability of eco-friendly gas under long-term or fault conditions. The replacement of incompatible materials or anti-corrosion treatment of solid interface might be conducted.

Biosafety

Utilization of insulating gas with low toxicity (ideally none) is required for biosafety concerns. The operation and maintenance personnel will inevitably need to contact eco-friendly gas during installation, maintenance, operation. Further, biosafety also determines its application feasibility, waste gas treatment and emission regulations. Besides, the decomposition of insulating gas may generate toxicity by-products, such as the H_2S, SO_2, SOF_2, SO_2F_2 produced by SF_6, which also pose potential risks. Thus, evaluation of the safety of eco-friendly insulating gas as well as the decomposition of by-products is necessary.

2.2 Classification of eco-friendly gas

In the 1980s, emerging research on the SF_6 substitute gas was initiated by equipment manufacturers such as General Electric (GE). As shown in Figure 3(b), Devins conducted sparking potential measurements for 35 kinds of electron affinity gases, pointing out that the insulation performance of CF_3—C≡C —CF_3, C_2F_5Cl, C_2F_5CN, C_4F_7N was superior to SF_6 when applied at 0.2 MPa[9]. Later, several novel gases with low GWP have been explored, which can be classified into the following categories.

Traditional gas

Traditional gas refers to the CO_2, N_2, air that commonly exists in daily life. It possesses the advantages such as excellent environmental features, low liquefaction temperature, and excellent biosafety, while its dielectric strength reaches only 30%~38% of SF_6[44]. Traditional gas is mainly employed as buffer gas and mixed with electron affinity eco-friendly gas for application currently. Specifically, there might exist synergistic effect between them[45,46]. That is, the dielectric performance of gas mixture is higher than the sum of the electric strengths by the mole fractions of its components. The positive synergistic effect is highly desired as the insulation performance of gas mixture will exceed all components. Besides, the utilization of traditional gas at higher working pressure (>0.7 MPa) to achieve better dielectric strength is another strategy for HV SF_6-free GIE.

Perfluorocarbons and trifluoroiodomethane

Research on PFCs mainly focuses on CF_4, C_2F_6, C_3F_8 and c-C_4F_8, while the first three belong to strong greenhouse gases. c-C_4F_8 has a dielectric strength 1.27 times of SF_6, the GWP of 8,700 and liquefaction temperature of −6°C[47,48], which needs to be mixed with CO_2, N_2 or air for application and exhibits little superiority with SF_6/N_2 gas mixture. Besides, the precipitation of carbon/graphene exists in c-C_4F_8 gas mixture after discharge[49,50]. Trifluoroiodomethane (CF_3I) has similar dielectric strength, lower GWP, atmospheric lifetime compared to c-C_4F_8[51,52]. However, the weak C—I bond in its molecular leads to the precipitation of solid iodine in discharges seriously[53,54]. In addition, CF_3I belongs to the carcinogenic, mutagenic, and reprotoxic (CMR) category, bringing potential safety hazards[55]. The existing drawbacks stopped the engineering application of PFCs and CF_3I.

Fluorinated-nitrile, ketones

In 2015, Minnesota Mining and Manufacturing (3M) presented fluorinated nitrile (C_4F_7N) and fluorinated ketones ($C_5F_{10}O$ and $C_6F_{12}O$) as the latest eco-friendly insulating gas[56,57]. Specifically, C_4F_7N has a dielectric strength of 2.2 times that of SF_6, a GWP of 2090, and an atmospheric lifetime of years. The ketones ($C_5F_{10}O$ and $C_6F_{12}O$) also demonstrate superior environmental features (GWP of 1) and dielectric strength (1.4 and > 2 times of SF_6). Owing to the relatively high liquefaction temperature, fluorinated nitrile and ketones have been introduced as admixtures to traditional gas for engineering application. The CO_2, technical air, O_2 is mainly utilized to obtain the binary or ternary gas mixture. For example, C_4F_7N/CO_2 with 6%, 10% C_4F_7N fulfills the minimum operating temperature of −25°C, −10°C (0.6 MPa), and the GWP value of gas mixture decreased to 462 and 690[56]. The fluorinated ketone based gas mixture is mainly used for MV GIE with 7%~14% $C_5F_{10}O$ or 3%~6% $C_6F_{12}O$ added[58,59]. For HV application, the mole fraction of ketones and the minimum operation temperature is further limited.

Hydrofluro-Olefins

Hydrofluro-Olefins (HFOs) are mainly used as refrigerants to replace the PFCs or saturated hydrofluorocarbons (HFCs) at present, in which HFO-1234ze(E), HFO-1336mzz(E) is proposed as eco-friendly insulating gas recently[60–62]. Specifically, HFO-1234ze(E) and HFO-1336mzz(E) have a GWP of 1 and 18, a dielectric strength of 0.81~0.98 and 1.63~1.86 times of SF_6, and a liquefaction temperature of −19.2°C and 7.58°C, respectively[63,64]. Thus, HFO-1234ze(E) can be used as pure gas in MV GIE down to −15°C. Besides, the acute toxicity of HFO-1234ze(E) has been systematically evaluated. Therefore, HFOs appear promising application potential for MV GIE that is mainly located in urban distribution networks, rail transit, buildings and other people crowded places.

Table 2 and Figure 3(c) summarized the basic parameters and development paths of eco-friendly insulating gas[10]. To date, it is still challenging to screen one gas with comprehensive performance as SF_6. There exists a trade-off or conflict between the environmental features and stability, dielectric strength and liquefaction temperature, etc.

2.3 Molecular design of eco-friendly gas

The key to designing new insulating gas is to predict its macro performance through the parameters at the molecular level. The general framework is shown in Figure 4. First, the possible gas molecular structure is preset, and then its performance is calculated

Table 2 The basic parameters of common eco-friendly insulating gas.

Chemical formula	Molecular structure	GWP (100 years)	Atmospheric lifetime (year)	Liquefaction temperature(°C)	Dielectric strength relative to SF_6 $(E/N)_{crit}$	LC50 (rat, 4 h, μL/L)
SF_6	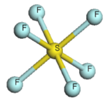	25,200	3,200	−64	1	—
CO_2	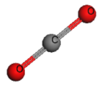	1	—	−78.5	0.35	—
N_2	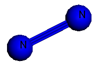	—	—	−196	0.38	—
O_2	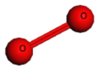	—	—	−183	0.33	—
CF_4	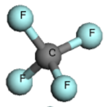	6,630	50,000	−128	0.41	—
c-C_4F_8	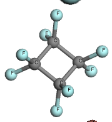	8,700	3,200	−6	1.27	—
CF_3I	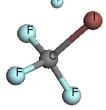	0.4	0.005	−21.8	1.2	160,000
HFO-1234ze(E)	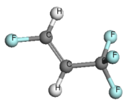	<1	0.045	−19.2	0.81~0.98	>207,000
HFO-1336mzz(E)	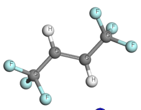	18	0.06	7.58	1.63~1.86	25,400–49,000
C_4F_7N	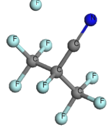	2,090	22	−4.7	2.2	12,500–15,000
$C_5F_{10}O$	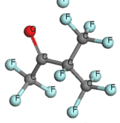	<1	0.044	26.9	1.4	20,000
$C_6F_{12}O$	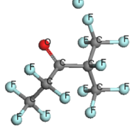	1	0.014	49	2.2	>100,000

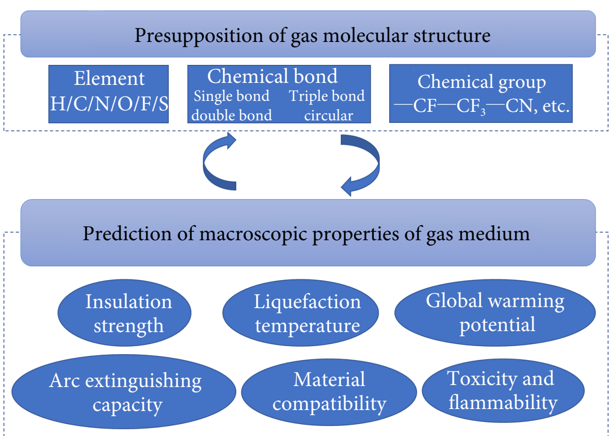

Fig. 4 General framework for molecular design of new insulating gases.

through an appropriate model. If the performance does not meet the requirements, the molecular structure is adjusted, and the gas molecules meeting the performance are obtained iteratively. In the process of molecular design, it is quite difficult to establish a performance prediction model due to missing data references. At present, the main prediction is for insulation strength or liquefaction temperature.

Performance prediction model

The first problem of the prediction model is how to select appropriate predictors. Most of the models reported at present directly give the predictors. Common insulation prediction factors are as follows:

(1) Ground state electric dipole momentum, average electric polarizability, and electronic affinity energy (EA)[65].

(2) Four predictors for polar molecules are electric dipole

moment, electron number, average static electronic polarizability, and adiabatic ionization energy. Four predictors for nonpolar molecules are average static electronic polarizability, adiabatic ionization energy, adiabatic electron affinity, and vertical electron affinity[66].

(3) Integral of the optical absorption (IOA)[67].

(4) The total surface area of the molecule, statistical variance, degree of balance, average deviation, molecular polarizability, absolute electronegativity, and hardness[68–71].

(5) Molecular diameter (van der Waals surface), 1st ionization energy, molecular electronegativity[72].

(6) Ionization energy, polarizability[73].

(7) General interaction properties function (GIPF) parameter of isosurface with electron localization function (ELF) of 0.2[74].

(8) Molecular volume, polar surface area, surface positive average potential, surface negative average potential, molecular polarity index[75].

(9) Molecular surface electrostatic potential, molecular volume, molecular surface area, polarizability[76].

(10) Electric dipole moment, positive surface area, average static electronic polarizability, molecular volume, highest occupied molecular orbital (HOMO), lowest unoccupied molecular orbital (LUMO), molecular mass[77].

Using these predictors and the reported insulation strength data, usually relative to the insulation strength of SF_6 gas, the corresponding relationship between the predictors and gas insulation strength can be established by regression analysis. In addition, these predictors can be obtained through density functional theory (DFT) calculation. In this way, the insulation strength of unknown gas can be predicted.

Characteristics of new gas

Through molecular design, gases that meet the requirements in theory can be obtained, and the performance needs to be determined through experiments. However, most of the designed gases cannot be bought and research on these gases can only depend on artificial synthesis. One typical example is the CF_3SO_2F proposed by Zhou et al., which has advantages in insulation, liquefaction through a prediction model and it was successfully synthesized in the laboratory[69,78]. Further, the electron swarm parameters of CF_3SO_2F gas were obtained by the steady-state Townsend (SST) experiment[79], and its dielectric strength under higher pressure was obtained through AC breakdown experiment[80]. Recently, the toxicity study of this gas has also reported preliminary results, indicating that CF_3SO_2F gas will be listed as a toxic compound by most standards[81]. This poses challenges for its application as an eco-friendly gas. It also shows that molecular design needs to consider multi-dimensional features, not only insulation or liquefaction.

3 Assessment of eco-friendly insulating gas

3.1 Dielectric properties

Dielectric properties are the foundation of eco-friendly insulating gas. Research on the insulation performance of eco-friendly insulating gas mainly focuses on its breakdown, PD, and surface flashover characteristics. The GIL or GIS has a coaxial structure that is dominated by a quasi-uniform electric field. Defects like protrusions or metallic particles also exist. Under different voltage forms and various electric fields, eco-friendly gases show different performance. Figure 5(a) depicts the methods and typical electrode system for the breakdown voltage measurement[82].

Alternating current (AC) breakdown

The AC breakdown voltage of PFCs with better insulating properties and low GWP values such as c-C_4F_8, C_3F_8, C_2F_6 have been tested[83]. Buffer gas such as N_2 or CO_2 is employed owing to the high boiling point. The synergistic effect between fluorocarbon main insulating and buffer gas should be considered, as it offers

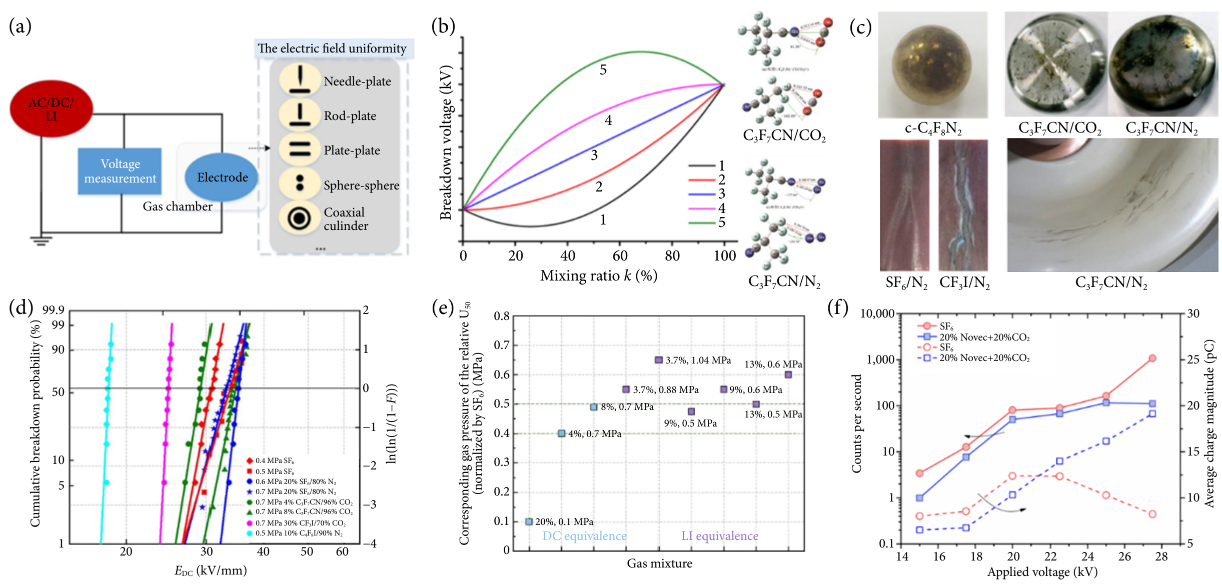

Fig. 5 The dielectric properties of eco-friendly insulating gases. **(a)** Diagram of the breakdown voltage measurement. Reprinted with permission from Ref. [83], © 2020 Author(s). **(b)** Synergy relationship of gas mixture: negative synergistic effect $C > 1$ (curves 1 and 2), linear relationship $C = 1$ (curve 3), and positive synergistic effect $C < 1$ (curves 4 and 5). Reprinted with permission from Refs. [83, 110], © 2019 Author(s). **(c)** The soot layer and trace on electrodes or insulators after gas discharge. Reprinted with permission from Refs. [19, 114], © 2018, IEEE. **(d)** The Weibull distribution of DC dielectric strength of various eco-friendly insulating gases. Reprinted with permission from Ref. [20], © 2021, IEEE. **(e)** Equivalence of breakdown voltages between C_4F_7N/CO_2 and SF_6 at DC and LI voltage. Reprinted with permission from Ref. [19], © 2020 Author(s). **(f)** The PD number and PD magnitude for the 20% C_4F_7N/CO_2 and SF_6 under different voltages. Reprinted with permission from Ref. [101], © 2018 IEEE.

additional insulation performance (Figure 5(b)). The insulation performance of the c-C_4F_8 gas under uniform electric field is 1.18~1.25 times than that of SF_6, and synergistic effect was found when PFCs combined with CO_2, N_2, CF_4, respectively[84–87]. The dielectric strength of gas mixture with 60% CF_3I can reach that of SF_6[88–90], and CO_2 possesses better synergistic effect than that of N_2[91,92]. However, the obvious solid by-product is generated (mainly includes I and C) under discharge (Figure 5(c)), which is very detrimental to gas self-recovery and mainly limits its application as the oxidation of materials due to the presence of iodine could not be ignored[53,54].

In 2015, Asea Brown Boveri (ABB) proposed the utilization of $C_5F_{10}O$ or $C_6F_{12}O$ in combination with technical air as insulating medium[93]. The breakdown voltage of the gas mixture containing 5.2% $C_5F_{10}O$ at 0.7 MPa can reach 95%, 80% of SF_6 at 0.45 MPa, 0.6 MPa. The addition of 3% $C_6F_{12}O$ to N_2 can bring double breakdown voltage of pure N_2[94,95]. It is considered that fluorinated ketone is more suitable for MV GIE owing to the relatively high liquefaction temperature. In 2016, GE reported the AC breakdown characteristics of C_4F_7N gas mixture for the first time[96]. The gas mixture with 20% C_4F_7N has similar dielectric strength to that of SF_6, and CO_2 or air demonstrates a better synergistic effect compared to that of N_2. The breakdown voltage of 3.7% C_4F_7N/96.3% CO_2 at 0.64 MPa, 0.76 MPa can reach the level of SF_6 at 0.55 MPa and 0.65 MPa[97–99].

HFOs such as HFO-1234ze(E), HFO-1336mzz(E) are also focused. The former has comparable insulation performance to SF_6 at 130 kPa[100]. The positive synergistic effect between HFO-1234ze(E) and SF_6 was found, and the gas mixture with 40%~60% HFO-1234ze(E) demonstrates 1.2 times dielectric strength of SF_6[101]. The AC breakdown voltage of HFO-1336mzz(E)/CO_2 with 25~30% HFO-1336mzz(E) can reach 75%~85% of SF_6 under the quasi-uniform electric field, and the relative dielectric strength can be significantly improved by increasing mixing ratio. There exists a favorable synergistic effect between HFO-1336mzz(E) and CO_2, and the breakdown voltage of HFO-1336mzz(E)/CO_2 mixture under the highly non-uniform electric field demonstrates a “hump” phenomenon with the increase of gas pressure, especially at 0.2 MPa[62].

Direct current (DC) Breakdown

The characteristics of gas under DC electric field are different from that of AC. The insulation performance of 20% CF_3I/80% N_2 and 30% CF_3I/70% N_2 at 0.15–0.25 MPa did not increase remarkably with gas pressure[20]. The negative DC dielectric strength of 4% C_4F_7N/96% CO_2, 8%C_4F_7N/92%CO_2 at 0.7 MPa reached 81.21% and 96.5% of SF_6 at 0.5 MPa, respectively[102,103]. Moreover, the DC insulation properties were found to be sensitive to the electrode surface roughness[104–106]. The DC breakdown voltage changed to saturation with the increase of gas pressure, especially for electrodes with larger surface roughness. The 6% C_4F_7N/94% CO_2 mixture was less sensitive to the electrode surface roughness than SF_6 and 20% SF_6/80% N_2(Figure 5(d))[106]. In addition, HFO-1336mzz(E)/CO_2 has a higher negative DC dielectric strength than HFO-1336mzz(E)/N_2, which can occupy 93.03% and 86.39% of 20%SF_6/80%N_2 at 0.7 MPa[107].

Defects like protrusions or metallic particles will lead to strong local non-uniform electric fields, resulting in a decrease in dielectric strength. It was reported that the DC breakdown characteristics of C_4F_7N/N_2 were strongly affected by polarity[106,108,109]. At the same gas pressure, the negative DC breakdown voltage was much higher than the positive, and their difference increased with pressure. The magnitude of the negative breakdown voltage increased with pressure, whereas the positive breakdown voltage displayed the opposite behavior.

Lightning impulse (LI) breakdown

The insulation characteristics of fluorocarbon gas also possess a polarity effect under lightning impulse breakdown. For example, the negative LI breakdown voltage of c-C_4F_8/N_2 was lower than that of positive. This was ascribed to the difference in free electrons’ speed and kinetic energy. The free electrons in a negative lightning strike had a higher velocity, making the gas molecules hard to capture. The synergistic effect of C_3F_8/N_2, C_2F_6/N_2 was found to be inferior to that of SF_6/N_2, so as to the CF_3I gas mixture[110]. The positive LI breakdown voltage of 5% $C_5F_{10}O$/95% air at 0.7 MPa reached that of pure SF_6 at 0.4 MPa[93,94]. For C_4F_7N, the LI insulation performance of 3.7% C_4F_7N/96.3% CO_2 at 0.88 MPa was equal to that of SF_6 at 0.55 MPa, and higher increase of pressure at 1.04 MPa brought little enhancement (reached SF_6 at 0.65 MPa)[97,111]. The equivalence of breakdown voltage between C_4F_7N/CO_2 and SF_6 gas at DC and LI voltage was summarized in Figure 5(e)[19].

Partial discharge

Fault-induced PD inside the GIE will cause electromagnetic radiation, noise, gas decomposition and materials deterioration. The gas insulating medium with superior PD withstand performance is highly desired. For PFCs, the partial discharge inception voltage (PDIV) of c-C_4F_8/N_2 with 15%~20% c-C_4F_8 reaches 65%~70% that of SF_6[112]. The PDIV of CF_3I/CO_2 was higher than that of CF_3I/N_2, and the 30% CF_3I/70% CO_2 was about 70% of SF_6 at 0.1 MPa[113]. The 20% C_4F_7N/80% CO_2 shows slightly higher PDIV with respect to SF_6, and SF_6 has much more PDs with low magnitude while C_4F_7N/CO_2 demonstrated fewer PDs with higher magnitude (Figure 5(f))[98,99]. The PDIV of C_4F_7N/CO_2 under an extremely non-uniform electric field demonstrated "hump effect", and the inhibition ability on negative PD is better than that of SF_6/N_2. For DC voltage, the negative polarity PDIV of C_4F_7N/CO_2 is higher than that of positive polarity, which is greatly affected by the non-uniformity coefficient of the electric field[114]. In addition, the $C_5F_{10}O$/air possessed higher PD amplitude under positive polarity, while for SF_6 it is under negative polarity.

Overall, fluorocarbon gas is proven to be sensitive to electric field inhomogeneity. The PD discharge repetition rate and average discharge magnitude of eco-friendly insulating gas with equivalent insulation performance to SF_6 are higher. The inhibition ability of negative PD is better than that of positive ones. In addition, the relative PDIV of fluorocarbon gas under high pressure is lower than that of low-pressure conditions. Considering that the proportion of buffer gases such as CO_2 with weak insulation performance is high, the PD characteristics are similar to CO_2 to some extent. In terms of engineering application, it is necessary to avoid the introduction of extremely uneven electric fields, and to strengthen PD monitoring and analysis in operation and maintenance.

Flashover

Surface flashover properties that are important and complex for gas-solid insulation design have also been evaluated. For PFCs, it was found that the flashover voltage of c-C_4F_8 was 1.2 times that of SF_6 with obvious polarity. The AC flashover voltage of CF_3I/N_2 is higher than that of SF_6/N_2, while it was lower under DC stress. For C_4F_7N, the AC surface flashover voltage of 9% C_4F_7N/91% CO_2

under 0.6 MPa could reach that of SF_6 at 0.5 MPa[115,116]. The negative DC flashover voltage of 4% C_4F_7N/96% CO_2, 8% C_4F_7N/92% CO_2 at 0.7 MPa were 96.06% and 101.50% of SF_6 at 0.5 MPa. In addition, the LI surface flashover voltage shows a saturated growth trend with pressure and mixing ratio, and the gas mixture with 5%, 9%, and 13% C_4F_7N can reach 70%, 80%, 90% of SF_6 under the same conditions. The surface discharge pattern in C_4F_7N/CO_2 and SF_6 has no obvious difference[116]. It should be noted that the accumulation of surface charge under DC conditions might cause electric field distortion, bringing specific surface flashover at lower voltage[117]. Relevant tests also found that the pot insulator flashover mostly occurred at the concave side, and the flashover voltage of 9% C_4F_7N/91% CO_2 at 0.6 MPa reached that of SF_6 at 0.5 MPa.

On the whole, current research has confirmed the superior insulation withstands characteristics of eco-friendly gases. Table 3 further summarized and compared the dielectric properties of various eco-friendly insulating gases. Relevant data provide important references for the design and optimization of GIE. For HV application scenario, the increase of gas pressure or minimum operating temperature (an increase of fluorocarbon gas content) is needed owing to their inferior dielectric strength. Meanwhile, the introduction of an inhomogeneous electric field should be avoided considering the reduction of relative insulation performance at high pressure. Further explorations on the synergistic effect mechanism should be addressed.

3.2 Arc-quenching

One of the essential elements to consider when applying eco-friendly gases in next-generation SF_6-free equipment is their arc-quenching ability. A good arc-quenching medium must present not only high thermal conductivity to cool the arc quickly but also high dielectric strength to facilitate the transient recovery voltage and to avoid the reignition of the arc[135]. To evaluate the arc-quenching performance of eco-friendly gases, many previous works have been done through numerical and experimental approaches.

Particle compositions

High-temperature arc is a kind of thermal plasma that has different particle compositions at different temperatures and pressures. The composition of an arc also plays an essential role in the calculation of arc plasma properties, such as thermodynamic properties and transport coefficients[136]. The computational results indicate that many eco-friendly gases, such as CF_3I[137], C_4F_8[138], C_4F_7N[139–141], and $C_5F_{10}O$[139,142–144], cannot recombine into itself after dissociation in arc plasmas. Most composition calculations assume that arc plasmas are at local thermodynamic equilibrium (LTE) and all species are gaseous. However, this is not always valid for eco-friendly gases. For instance, C_4F_7N and $C_5F_{10}O$ can produce condensed species, i.e., graphite in arc plasmas (Figure 6(a)), and the condensation temperature of graphite decreases more or less with the increase of buffer gases[142,145]. To yield graphite-free products at room temperature, O_2 can be mixed with C_4F_7N and $C_5F_{10}O$ mixtures to completely constrain the production of graphite[139]. Since the condensed species exist only at low temperatures, it is necessary to consider the departure from LTE, which requires the calculation of non-LTE two-temperature (2T) plasma compositions [146,147]. It is found that the condensation temperatures of condensed species in eco-friendly gaseous arcs do not vary monotonously with the non-equilibrium degree in arc plasmas, and the balance effect can be observed between electron temperature T_e and heavy particle temperature T_h at low value of non-equilibrium degree[139].

Thermodynamic properties

Based on the particle compositions, the thermodynamic properties including mass density, specific heat, enthalpy, entropy, etc., can be calculated directly according to their thermodynamic definitions[147]. Generally, a gas with high specific heat has good ability to cool the hot arc during the arc extinction. In comparison to SF_6, $C_5F_{10}O$ and $C_5F_{10}O$-CO_2 mixtures present higher specific heat except in the medium temperature range[142]. Some previous works reveal that the thermal interruption performance of a gas can be evaluated by the temperature dependence of the product of specific heat and mass density (i.e., ρC_p)[137,148]. C_4F_8-CO_2 arc shows higher peaks of ρC_p at high temperatures and lower peaks at low temperatures than SF_6[138]. $C_5F_{10}O$ arc presents a similar characteristic[143]. It is also found that the mixing of buffer gases (e.g., N_2 and CO_2) can gradually erase the peaks of ρC_p in the C_4F_7N arc (Figure 6(b))[141], which inevitably affects the arc cooling rate during the arc-quenching process. Most previous works on the thermodynamic properties of eco-friendly gases only consider gaseous species. However, the production of graphite in $C_5F_{10}O$ arc has an influence on the mass density and specific enthalpy in the low-temperature range[142].

Transport coefficients

Arc plasma modeling requires not only thermodynamic properties but also transport coefficients. The transport coefficients including electrical conductivity, viscosity, and thermal conductivity can be determined by the collision integrals based on the Chapman-Enskog method[149]. The condensed species in the arc plasmas of eco-friendly gases, e.g., graphite, are usually neglected in calculating collision integrals and transport coefficients. Since eco-friendly gases are large molecules that have rich products in arc plasmas, many complex chemical reactions have to be considered in the calculation of thermal conductivity. These reactions especially the dissociation and ionization reactions lead to peaks of thermal conductivity[138,140,143,144]. The arc cooling rate strongly depends on the peaks of thermal conductivity, particularly on the peak at the highest temperature. The arc decays fast above this highest temperature and slowly below this temperature[150]. The mixing of buffer gases, such as CO_2, N_2, and O_2, also has an effect on the transport coefficients of eco-friendly gaseous arcs (Figure 6(c)). For example, the mixing of CO_2 or N_2 shows a significant effect on the viscosity of C_4F_8-CO_2, C_4F_7N-CO_2, and C_4F_7N-N_2 arcs[138,140]. However, the buffer gases do not show a distinct influence on the electrical conductivity of C_4F_7N arcs if only small proportion of buffer gas is mixed[140].

Radiation coefficients

Radiation plays an import role in arc extinction. In high-voltage circuit breakers (HVCBs), the energy loss due to radiation increases the cooling rate of the arc during the current zero and is responsible for the ablation of the nozzle[138]. Therefore, the radiation properties of an arc are required to understand the arc decaying process[140]. However, solving radiation transport equations is rather complicated and time-consuming, as the radiation transfer strongly depends on the computational geometry and gas types, and is a function of wavelength spanning from the infrared to the far ultraviolet region of the spectrum[138]. As a result, a simplified model, namely net emission model, is usually used in arc modeling. The corresponding coefficients in this model are net emission coefficients (NEC) which can be calculated by considering all the atomic and molecular radiations in arc plasmas[151–154]. It is found that the NEC of C_4F_8-CO_2 arcs is slightly larger than that of SF_6[138].

Table 3 The dielectric properties of eco-friendly insulating gas under different voltage types.

Gas	Voltage type	Dielectric properties
c-C_4F_8	AC	✦ Sphere-plate electrode, 0.2–0.5 MPa, 50% *c*-C_4F_8/50% N_2, 90% that of SF_6[118]. ✦ Sphere-plate electrode, 0.1 MPa, 20% *c*-C_4F_8/80% N_2 or CO_2, 67%(N_2), 68%(CO_2) that of SF_6; 30% c-C_4F_8/70% N_2 or CO_2, 0.1 MPa, 75%(N_2), 79%(CO_2) that of SF_6[119].
		✦ Neelde-plate electrode, 0.1–0.3 MPa, 20% *c*-C_4F_8/80% N_2, 60%–90% that of 20%SF_6/N_2[120].
	LI	✦ Sphere-plate electrode, 0.1 MPa, 10% *c*-C_4F_8/90% N_2 or CO_2, positive LI breakdown voltage higher than that of negative, 60% that of SF_6[121].
	DC	✦ Sphere-plate electrode, 0.1–0.5 MPa, 20% CF_3I/80% N_2, 62% that of SF_6; 10% CF_3I/90% N_2, 43% that of SF_6[122].
	Surface flashover	✦ AC, 0.1 MPa, 30% *c*-C_4F_8/70% N_2, 73% that of SF_6[123].
		✦ DC, 0.1–0.5 MPa, 20% CF_3I/80% N_2, 71% that of SF_6; 10% CF_3I/90% N_2, 65% that of SF_6[122].
CF_3I	AC	✦ Sphere-plate electrode, 0.1–0.3 MPa, 30% CF_3I/70% N_2, 92%–98% that of SF_6[124]. ✦ Needle-plate, 0.3 MPa, 30% CF_3I/70% N_2, 85%–90% that of SF_6[88].
	LI	✦ Needle-plate electrode, 0.1–0.3 MPa, 30% CF_3I/70% N_2, lower than 20% SF_6/80% N_2 (80%–86%)[110].
	DC	✦ Plate-plate electrode, 0.1–0.2 MPa, 30% CF_3I/70% N_2, similar to that of 20% SF_6/80% N_2[91].
	Surface flashover	✦ LI, 0.1–0.3 MPa, 30% CF_3I/70% N_2, similar to 20% SF_6/80% N_2 under negative LI, higher than 20% SF_6/80% N_2 under positive LI[110].
C_4F_7N	AC	✦ Plate-plate electrode, 0.1–0.7 MPa, 13%C_4F_7N/87%CO_2, >90% that of SF_6; 9%C_4F_7N/91%CO_2, >80% that of SF_6[125]. ✦ Sphere-sphere electrode, 0.1–0.3 MPa, 8% C_4F_7N/92% CO_2, 72.8%(0.3 MPa)–76.5%(0.1 MPa) that of SF_6[99]. ✦ Needle-plate electrode, 0.1–0.3 MPa, 8% C_4F_7N/92% CO_2, 68.3%(0.3 MPa)~71.6% (0.1 MPa) that of SF_6[97].
	LI	✦ Plate-plate electrode, 0.5–1.0 MPa, 3.7% C_4F_7N/96.3%CO_2 at 0.88 MPa, 1.04 MPa reach that of SF_6 at 0.55 MPa, 0.65 MPa[126]. ✦ Needle-plate electrode, 0.1–0.4 MPa, 10% C_4F_7N/90% CO_2, 80% that of SF_6(positive LI), 75% that of SF_6(negative LI) [102].
	DC	✦ Sphere-plate electrode, 0.3–0.7 MPa, 4% C_4F_7N/96%CO_2(0.7 MPa), 8% C_4F_7N/92%CO_2 (0.7 MPa) reaches 75.05%, 81.21% that of SF_6 (0.5 MPa) (negative DC)[26]. ✦ Needle-plate electrode, 0.3–0.7 MPa, positive DC breakdown voltage of 8% C_4F_7N/92%CO_2 is lower than 4% C_4F_7N/96%CO_2 (polarity effect) [27].
	Surface flashover	✦ AC, 0.1–0.5 MPa, C_4F_7N/CO_2 with 5%, 9%, 13%, 17% C_4F_7N reaches 70%, 75%, 80%, and 85% of SF_6[103].
$C_5F_{10}O$	AC	✦ Rod-plate electrode, 0.2–0.55 MPa, $C_5F_{10}O$/CO_2 with 20 kPa, 40 kPa $C_5F_{10}O$ rechaes 61.89%, 81.99% of SF_6 at 0.2 MPa[127]. ✦ Sphere-sphere electrode, 0.1–0.5 MPa, $C_5F_{10}O$/N_2 and $C_5F_{10}O$/air with 45 kPa $C_5F_{10}O$ reaches 84%, 91% that of SF_6[128].
	LI	✦ Rod-plate electrode, 0.2–0.55 MPa, $C_5F_{10}O$/CO_2 with 20 kPa, 40 kPa $C_5F_{10}O$ at 0.5 MPa rechaes 88.9%, 89.9% of SF_6 at 0.3 MPa[128]. ✦ Plate-plate electrode, 0.1–0.2 MPa, $C_5F_{10}O$/air or $C_5F_{10}O$/CO_2 with 28% $C_5F_{10}O$ is litter higher than that of SF_6. $C_5F_{10}O$/air (0.166 MPa) or $C_5F_{10}O$/CO_2 (0.114 MPa) with 10% $C_5F_{10}O$ reaches that of SF_6 at 0.1 MPa[129].
	SI	✦ Needle-plate electrode, 0.1–0.5 MPa, negative SI of $C_5F_{10}O$/CO_2 with 2%–8% $C_5F_{10}O$ is higher than that of positive, reaching 60%–70% that of SF_6[130].
	DC	✦ Rod-plate electrode, 0.1–0.3 MPa, $C_5F_{10}O$/CO_2 with 20 kPa $C_5F_{10}O$, 75%(0.3 MPa)~90%(0.1 MPa) that of SF_6[131].
$C_6F_{12}O$	AC	✦ Sphere-sphere electrode, 0.1–0.3 MPa, $C_6F_{12}O$/N_2 with 6% $C_6F_{12}O$, 1.03–1.11 times of 10% SF_6/90% N_2. $C_6F_{12}O$/N_2 with 6% $C_6F_{12}O$, 1.10–1.35 times of 10% SF_6/90% CO_2[95].
HFO-1234ze(E)	AC	✦ Sphere-plate electrode, 20% HFO1234ze(E)/80% N_2, 57%–74% that of 20% SF_6/80% N_2; Needle-plate electrode, 20% HFO1234ze(E)/80% N_2, 92%–98% that of 20% SF_6/80% N_2[132]. ✦ Hemisphere-plate electrode, most of breakdowns on positive half cycle[133].
	LI	✦ Needle-plate electrode, 0.1–0.3 MPa, pure HFO1234ze(E), 74% that of SF_6 at 0.1 MPa, 94% of SF_6 at 0.3 MPa[134].
	DC	✦ Plate-plate electrode, pure HFO1234ze(E), 83% that of SF_6[134].
HFO-1336mzz(E)	AC	✦ Sphere-sphere electrode, 0.1–0.3 MPa, 25% HFO-1336mzz(E)/75% CO_2 reaches 64%(0.1 MPa)–76%(0.2 MPa) that of SF_6; 30% HFO-1336mzz(E)/70% CO_2 reaches 71%(0.1 MPa)–85%(0.2 MPa) that of SF_6[62]. ✦ Needle-plate electrode, 0.1–0.3 MPa, HFO-1336mzz(E)/CO_2 with 25%, 30% HFO-1336mzz(E) reaches 102%–105% that of SF_6; "hump" phenomenon exits with the peak at 0.2 MPa[107].
	DC	✦ Plate-plate electrode, 0.1–0.5 MPa, HFO-1336mzz(E)/CO_2 with 10%, 20% HFO-1336mzz(E) reches 58%, 67% that of SF_6; HFO-1336mzz(E)/N_2 with 10%, 20% HFO-1336mzz(E) reches 51%, 63% that of SF_6[107].

For the role of buffer gases, it is observed that the NECs of C_4F_7N-N_2 and C_4F_7N-CO_2 arcs are very close to that of C_4F_7N arc until the buffer gas proportion reaches 50% (Figure 6(d))[140]. In general, the works on calculating radiation coefficients of eco-friendly gaseous arcs are not as much as those on the thermodynamic and transport coefficients. One of the likely explanations is the lack of atomic and molecular spectrum data and the cross sections of collision processes.

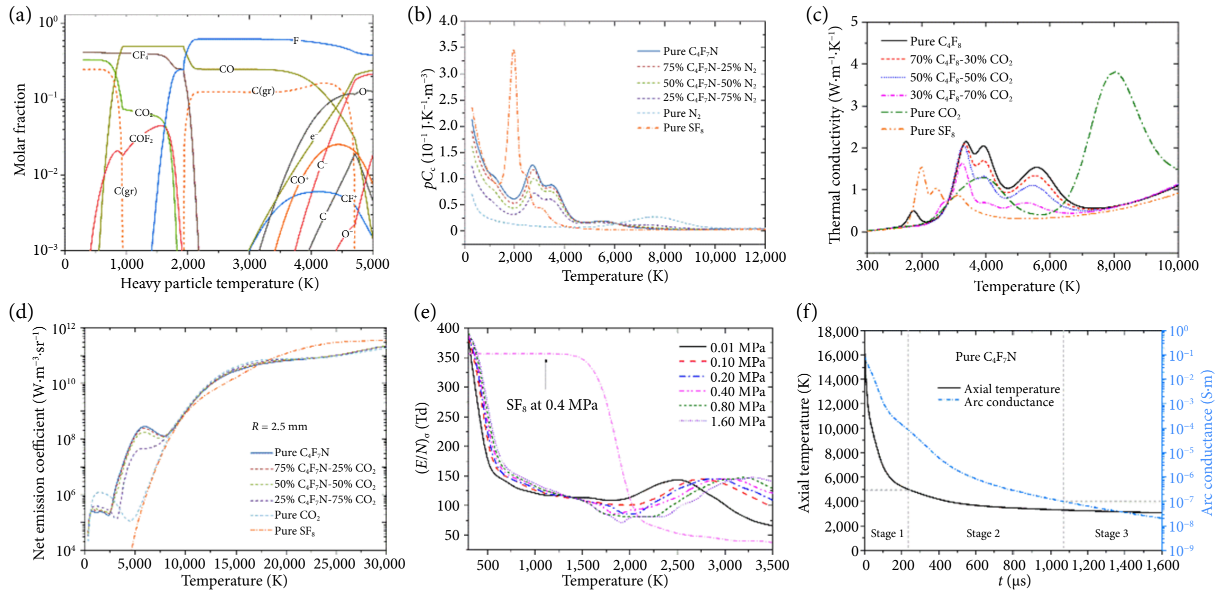

Fig. 6 Basic data of eco-friendly gaseous arcs. (a) Particle compositions. Reprinted with permission from Ref. [141], © 2021 Wiley-VCH GmbH. **(b)** Thermodynamic properties. Reprinted with permission from Ref. [142], © 2019 Springer Science Business Media, LLC, part of Springer Nature. **(c)** Transport coefficients. Reprinted with permission from Ref. [140], © 2018 AIP Publishing. **(d)** Radiation coefficients. Reprinted with permission from Ref. [142], © 2019 Springer Science Business Media, LLC, part of Springer Nature. **(e)** Dielectric breakdown properties. Reprinted with permission from Ref. [160], © 2015, EDP Sciences, SIF, Springer-Verlag Berlin Heidelberg. **(f)** Arc decaying characteristics. Reprinted with permission from Ref. [142], © 2019 Springer Science Business Media, LLC, part of Springer Nature.

Post-arc dielectric breakdown properties

During the arc interruption process, a high electric field strength caused by a transient recovery voltage (TRV) is applied to the hot gaseous medium between electrodes. If the hot gas has a lower dielectric strength than the applied electric field strength, the gas breakdown will occur, leading to the re-ignition of the arc[155]. In this case, the insulating gases remain a much higher temperature than room temperature during the arc extinction[156]. It is therefore necessary to investigate the dielectric breakdown properties of hot gas mixtures rather than cold gases at room temperature. This is usually achieved by the analysis of Boltzmann equation which describes the electron transport in hot gases. Bolsig+ is the widely used toolkit for solving the Boltzmann equation of weakly ionized gases[157]. In addition, the particle compositions at the temperatures considered and the electron-impact cross sections including elastic, ionization, electron attachment and excitation cross sections are needed in the calculation[155,156,158]. Most previous works on this topic are devoted to SF_6 and its various mixtures[156,159,160]. Very few works focus on eco-friendly gases, except for C_3F_8[158]. It is found that hot C_3F_8 gas has much poorer dielectric breakdown performance than SF_6(Figure 6(e))[158].

Evaluation of arc-quenching performance

The arc-quenching performance is usually evaluated by means of numerical modeling or experiments. The former approach is generally cheaper than the latter one. Based on the thermodynamic properties, transport coefficients, and radiation coefficients, a computational fluid model, namely magnetohydrodynamics (MHD) model can be established to describe arc characteristics and thus evaluate arc interruption ability. CO_2 has been investigated by the MHD modeling that it has a lower arc core temperature and larger arc radius than SF_6[161]. Using the same method, the arc-quenching performance of C_4F_7N-CO_2 and $C_5F_{10}O$-CO_2 mixtures has been compared with pure SF_6 and CO_2 (Figure 6(f))[162]. Considering that 2-D and 3-D MHD modeling are always time-consuming, 1-D modeling is used in investigating the decaying characteristics of CF_3I and C_4F_7N arcs[140]. For instance, the result of the 1-D arc model indicates that CF_3I shows a higher performance of thermal interruption than CO_2, N_2 and air[163]. To further reveal the arc interruption ability in a more sophisticated way, a fast evaluation method is proposed by combining 1-D hydrokinetic modeling and Boltzmann equation analysis[135,164]. However, due to the lack of electron-impact cross sections, this method is only applied to evaluate the arc-quenching performance of SF_6, CF_4, CO_2, and air. In addition to numerical works, some researchers performed experimental investigations on the arc-quenching of eco-friendly gases by measuring arc voltage, current, and emission spectrum. They found that $C_5F_{10}O$-CO_2 arc is more volatile than SF_6 gas, and adding $C_5F_{10}O$ into CO_2 can improve the stability of the arc, and significantly reduces the arc temperature[165]. C_4F_7N and its mixtures with CO_2 are also tested experimentally in a disconnector, and the results show that the arcing time is stable over 100 operations[96].

3.3 Stability and decomposition

Eco-friendly insulating gas will decompose to low carbon or fluorine fractions under discharges or over-thermal faults. These products have inferior dielectric strength and will not fully recombine to the original molecules, which may severely decrease the insulation and interruption capacity of gas. Therefore, the decomposition characteristics of eco-friendly gas is important in evaluating the operating feasibility, which has been explored in thermal, discharge aspects as well as theoretical level.

Thermal decomposition

The current heat effect or poor contact induced partial over-thermal fault (POF) are the main reason for thermal decomposition. Recent studies have clarified the thermal decomposition conditions, by-product type and content of eco-friendly insulating gas. For example, the initial decomposition temperature of pure gaseous C_4F_7N (test conducted based on Tubular furnace) reaches 500–650°C, and CF_3CN, C_3F_6, C_2F_5CN are detected by Fourier

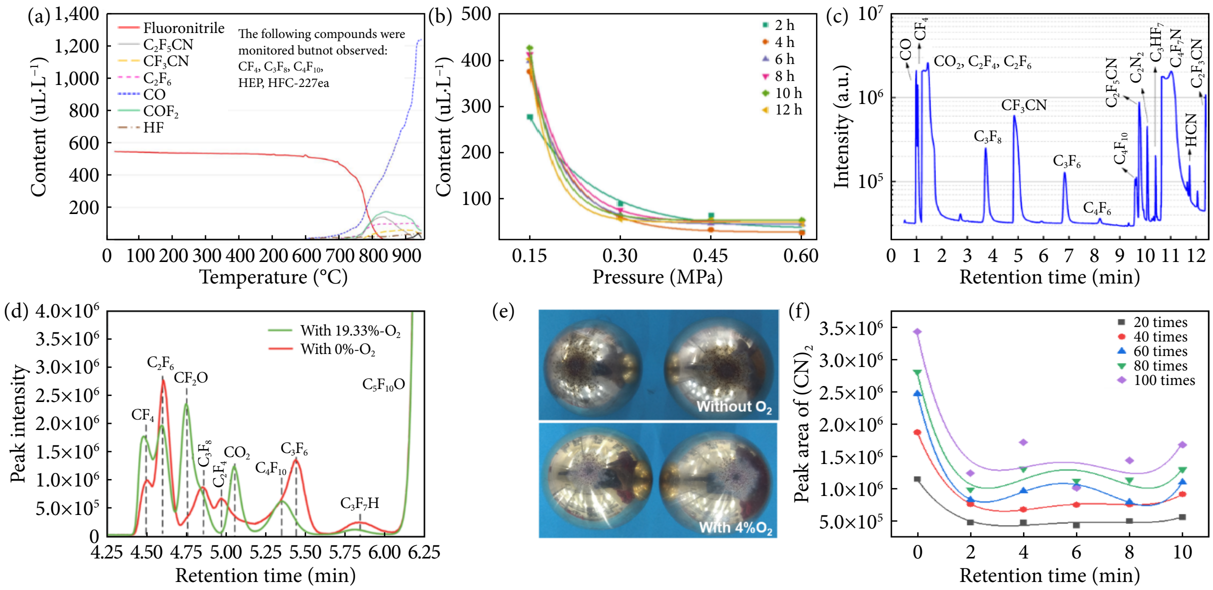

Fig. 7 The thermal and discharge decomposition properties of eco-friendly insulating gas. (a) Decomposition products from thermal degradation of C_4F_7N. Reprinted with permission from Ref. [57], © 2016 IEEE. **(b)** The C_3F_6 generated by C_4F_7N/CO_2 thermal decomposition at 450°C under different pressures. Reprinted with permission from Ref. [169], © 2020 Author(s). **(c)** The decomposition products of C_4F_7N/CO_2 after multiple breakdowns. Reprinted with permission from Ref. [172], © 2019 AIP Publishing. **(d)** The decomposition products of $C_5F_{10}O/N_2/O_2$ after multiple breakdowns. Reprinted with permission from Ref. [181], © 2019 Author(s). **(e)** The electrode morphology of C_4F_7N/N_2 gas mixture after multiple breakdowns. Reprinted with permission from Ref. [182], © 2019 IEEE. **(f)** The influence of O_2 content on the yield of C_2N_2. Reprinted with permission from Ref. [182], © 2019 IEEE.

infrared spectrometer (FTIR) or gas chromatography-mass spectrometer (GC-MS)[56,166,167]. Other by-products such as CO, C_2F_4, C_2F_6, C_3F_8 and C_2N_2 are generated at higher temperature (700°C) (Figure 7(a))[56]. The utilization of metal thermocouples for POF simulation obtained lower initial decomposition temperature (~350°C), which is ascribed to the participation of the metal interface[167]. Specifically, C_3F_6 is first detected, followed by C_2N_2, CF_4, C_3F_8, etc. The fluorinated ketones demonstrate similar thermal decomposition properties, and the by-products including CF_4, C_2F_6, C_3F_8, C_3F_6, C_3F_7H, C_5F_{12} are generated[168].

Besides, the gas pressure plays an important role in thermal decomposition. The amount of various decomposition products decreases with the increase of gas pressure and tends to be stable at ~0.3 MPa (Figure 7(b))[167]. This is because the increase of gas dissociation reaction rate constant is less than linear with the pressure[166]. Thus, the thermal stability of eco-friendly insulating gas at higher pressure is superior, which favors the HV-GIE application. Besides, the addition of >6% O_2 demonstrates a negative impact on thermal stability[169]. The formation of C_3F_8, C_3F_6, CF_3CN, C_2F_5CN and C_2N_2 is inhibited while the content of CF_4, COF_2 increases. Further investigation on the influence of trace impurities (such as H_2O) on the thermal stability and the gas aging mechanism under electrothermal conditions is necessary.

Discharge decomposition

The discharge decomposition of eco-friendly insulating gas is mainly caused by collision ionization, photoionization and thermal ionization, and various fractions (positive, negative ions, neutral particles) will be generated. Meanwhile, the fractions will react with each other to form decomposition by-products. The PD, dielectric breakdown, arc-quenching, etc. cause decomposition of eco-friendly gases. For C_4F_7N gas mixture, common by-products including CO, CF_4, C_2F_6, C_2F_4, C_3F_8, C_3F_6, CF_3CN, C_2N_2, C_2F_5CN, C_4F_8 are detected (Figure 7(c))[170,171]. For fluorinated ketones, CO_2, CF_4, C_2F_6, C_2F_4, C_3F_8, C_3F_6, C_3F_7H, C_4F_{10}, C_5F_{12}, C_6F_{14}, C_4F_8 are generated (Figure 7(d))[172–179]. The dielectric strength of most decomposition by-products is inferior to that of electron affinity gas, and the C_4F_8, CF_3CN, C_2F_5CN, C_2N_2, C_3F_6, COF_2, HF, HCN belongs to corrosive or toxic substances, which may pose a potential threat to insulation stability and maintenance personal safety.

Importantly, current experiments confirm that the generated fractions cannot fully recombine to electron affinity gas itself after discharge, which is ascribed to the complex molecular structure with low symmetry. There also exists a "cumulative effect" of the generated by-products. That is, the yield of various by-products shows a linear growth trend with the discharge intensity, period, and the electron affinity gas in the mixture is constantly consumed. The mixing ratio should be monitored to avoid the impact of insulation degradation caused by continuous consumption of electron affinity gas on GIE operation reliability. Besides, the formation or participation of solid by-product exists for fluorocarbon eco-friendly insulating gas, especially when N_2 is employed as the buffer gas (Figure 7(e))[180]. The addition of O_2 is capable of inhibiting the most gaseous and solid decomposition by-products (Figure 7(f))[180–182]. On one hand, O_2 has a preferable arc-quenching capability than CO_2 or N_2, which causes faster decaying rate of arc conductivity[181,182]. On the other, the carbon particles generated by arc discharge can be oxidized to CO or CO_2 by O_2 during discharge[182]. It should be noticed that higher content of O_2 brings negative effect on gas stability. It is necessary to establish the correlation between discharge and decomposition properties, as well as to explore the suppression scheme of by-products to further improve the stability of eco-friendly insulating gas.

Decomposition mechanism

Understanding the decomposition mechanism is significant for gas performance optimization. The development of quantum chemistry and multi-physics simulation promotes relevant research. The generation/loss rate of by-product is determined by chemical reactions and the initial concentration according to mass action law, which should be investigated in chemical kinetics

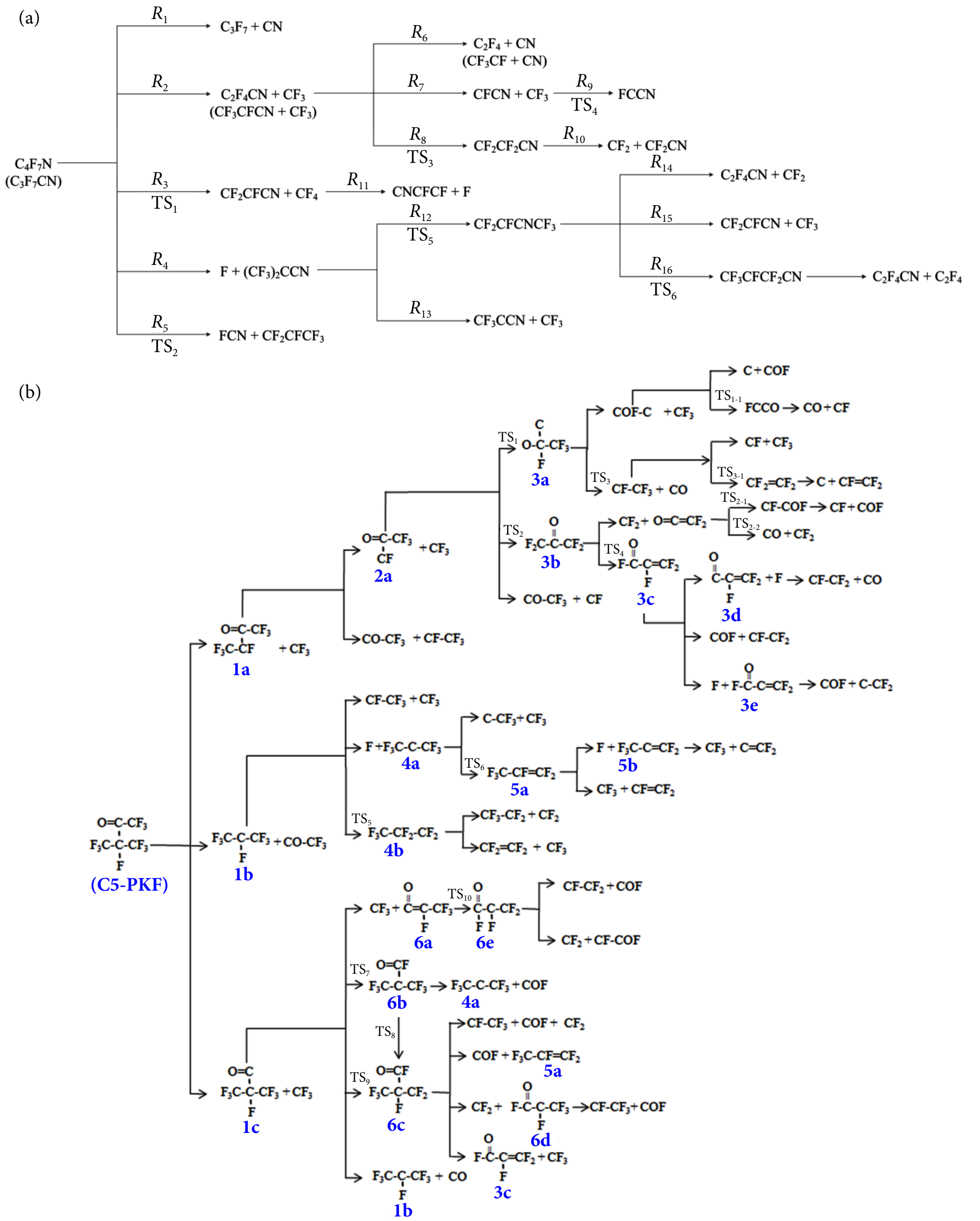

Fig. 8 The decomposition scheme and reaction pathways of eco-friendly insulating gas. (a) C_4F_7N. Reprinted with permission from [185], © 2019 IOP Publishing. **(b)** $C_5F_{10}O$. Reprinted with permission from [187], © 2016 Author(s).

model with a complete set of reactions. The relatively-complete decomposition scheme and reaction pathways of eco-friendly gases (such as C_4F_7N and $C_5F_{10}O$) are shown in Figure 8[183–185]. The potential energy surface of various reactions can be obtained by DFT and transition state (TS) calculations (Figures 9(a)–9(d)). For C_4F_7N, a slight barrier height in reaction R_1 ($C_4F_7N \rightarrow C_3F_7$ + CN) exists, which is less likely to occur than reaction R_2 ($C_4F_7N \rightarrow C_2F_4CN + CF_3$) and R_4 ($C_4F_7N \rightarrow F + (CF_3)_2CCN$). The reaction R_5 ($C_4F_7N \rightarrow$ TS2 $\rightarrow$ FCN + CF_2CFCF_3) is more likely to occur than reaction R_3 in C_4F_7N dissociation(Figure 9(a)). Besides, R_5 is the most important reaction leading to the dissociation of C_4F_7N below 600 K with larger reaction constants, while reaction R_2 takes the place of reaction R_5 over 600 K to 3,300 K and reaction R_3 become dominant above 700 K (Figure 9(b))[183]. For $C_5F_{10}O$, the favorable decomposition reactions include C–C bond ruptures producing **1a** and **1b**, followed by subsequent C–C bond ruptures and internal F atom transfers in the decomposition of **1a** and **1b**, respectively(Figures 9(c) and 9(d))[185].

Moreover, chemical kinetic models including local thermodynamic equilibrium (LTE) and non-local chemical equilibrium (non-LCE) can be used to explore the gas composition, as summarized in Section 3.2. The ReaxFF molecular dynamics (ReaxFF-MD) is also proposed to explore the decomposition process of eco-friendly gas[186–190]. The bond cleavage and formation during chemical reactions are described by the ReaxFF force field, which can be optimized by DFT[187]. The main particle including CF_3, CF_2, CF, CN, F, CNF, C_3F_7, C_3NF_4, C_4NF_6, CF_4 etc. are generated in C_4F_7N, $C_5F_{10}O$, $C_6F_{12}O$ gas mixture (Figure 9(e))[186–190]. Besides, the

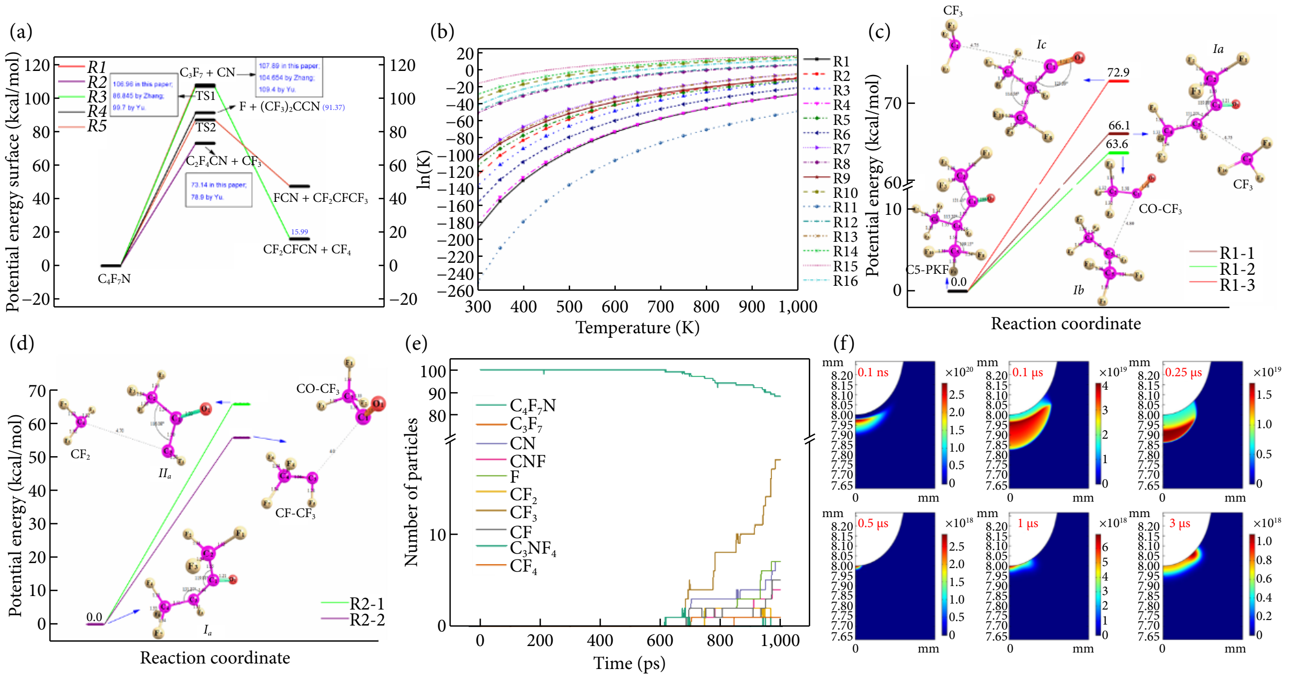

Fig. 9 The decomposition mechanism of eco-friendly insulating gas. (a) Decomposition potential energy surface of C_4F_7N including reactions R_1-R_5. Reprinted with permission from Ref. [185], © 2019 IOP Publishing. **(b)** Rate constants of C_4F_7N decomposition reactions during 300–1,000 K. Reprinted with permission from Ref. [185], © 2019 IOP Publishing. **(c)** Decomposition potential energy surface of $C_5F_{10}O$ (generating Ia and Ib). Reprinted with permission from Ref. [187], © 2016 Author(s). **(d)** Decomposition potential energy surface of Ia. Reprinted with permission from Ref. [187], © 2016 Author(s). **(e)** Time evolution of the C_4F_7N decomposed major species at 1,900 K. Reprinted with permission from Ref. [188], © 2017 Author(s). **(f)** Distribution of positive ion density near the discharge electrode in C_4F_7N/CO_2. Reprinted with permission from Ref. [193], © 2022 Author(s).

numerical simulation model of chemical kinetics-fluid is proposed to explore the PD decomposition mechanism insulating gas. For C_4F_7N, the 2D axisymmetric model combines the drift-diffusion and Poisson's equations were used and the distribution of positive, negative ions and electrons were obtained (Figure 9(f))[191]. Further research on the regulation of decomposition by-products generation and inhibition of solid precipitation mechanism needs to be clarified based on the above-mentioned schemes.

3.4 Materials compatibility

Assessment on the materials compatibility of eco-friendly gas has been focused on metals, epoxy resin, elastomers, adsorbent (or desiccant) currently. The aging tests were conducted at specific period or temperature, followed by the gas composition and solid materials properties analysis[192,193]. Besides, DFT or molecular dynamics (MD) studies were conducted to further reveal the gas-solid interface interaction mechanism[194].

Metal

The compatibility between fluorinated-nitrile, ketones, and HFO-1234ze(E) with copper, aluminum, silver has been evaluated. Copper demonstrated poor stability when contacted with C_4F_7N, $C_5F_{10}O$, and $C_6F_{12}O$ at 120–220°C[195–200]. The copper surface was corroded with fluoride accumulation, and the generation of C_3F_6 and C_3F_7H was found (Figure 10(a))[201–203]. Further analysis confirmed that the square planar copper(II) complex with two perfluorinated N-acylamidine ligands was formed during the multi-step interface reaction(Figure 10(b))[204]. The interaction between fluorinated-nitrile, ketones and aluminum, silver had little influence while the formation of C_3F_6 existed at high interface temperature. Besides, the PD induced decomposition also results in copper corrosion or fluorocarbon solid by-product precipitation, as shown in Figure 10(c)[204].

The interaction mechanism of fluorinated nitrile, ketone with metal is also investigated. The interaction energy and electronic parameters such as charge transfer, density of states were revealed based on DFT. Specifically, relevant evaluations on the Cu, Al, Ag, Zn, and ZnO surfaces confirmed the strong interaction activity of –CN, and –C=O group of C_4F_7N, $C_5F_{10}O$ and $C_6F_{12}O$. The obvious electron charge transfer and bonding were found (Figures 10(d) and 10(e))[205,206]. The adsorption-dissociation process was also explored, indicating the metal acts as the catalytic interface for gas decomposition. The formation of C_3F_6 might be ascribed to this. Overall, anti-corrosion treatment of copper is needed for fluorinated-nitrile, ketone based GIE. Future exploration on the metal alloy, anti-corrosion coating as well as the impact of gas-metal interaction process on the electrical, thermal conductivity should be clarified.

Epoxy resin

Epoxy resin is normally used as solid insulating material in GIE. The compatibility assessment on C_4F_7N/CO_2 found that the DC conductivity of epoxy resin decreased with the aging temperature, while AC conductivity demonstrates an increasing trend[207]. The surface flashover voltage was kept stable after interaction. Higher aging temperature (>160°C) resulted in the formation of C_3F_6 and $C_{12}F_{21}N_3$. The C_4F_7N-epoxy resin interface discharge decomposition properties were also investigated[208,209]. Various by-products including CF_4, C_3F_8, C_6F_{14}, C_3F_6, C_4F_6, C_4F_8, CF_3CN, and $C_{12}F_7H_{17}O_2$ were detected, which content increased with the PD period. Moreover, –CF and –CN were found on the epoxy resin surface. Further explorations on the interaction properties between eco-friendly gas and the main decomposition by-products should be conducted.

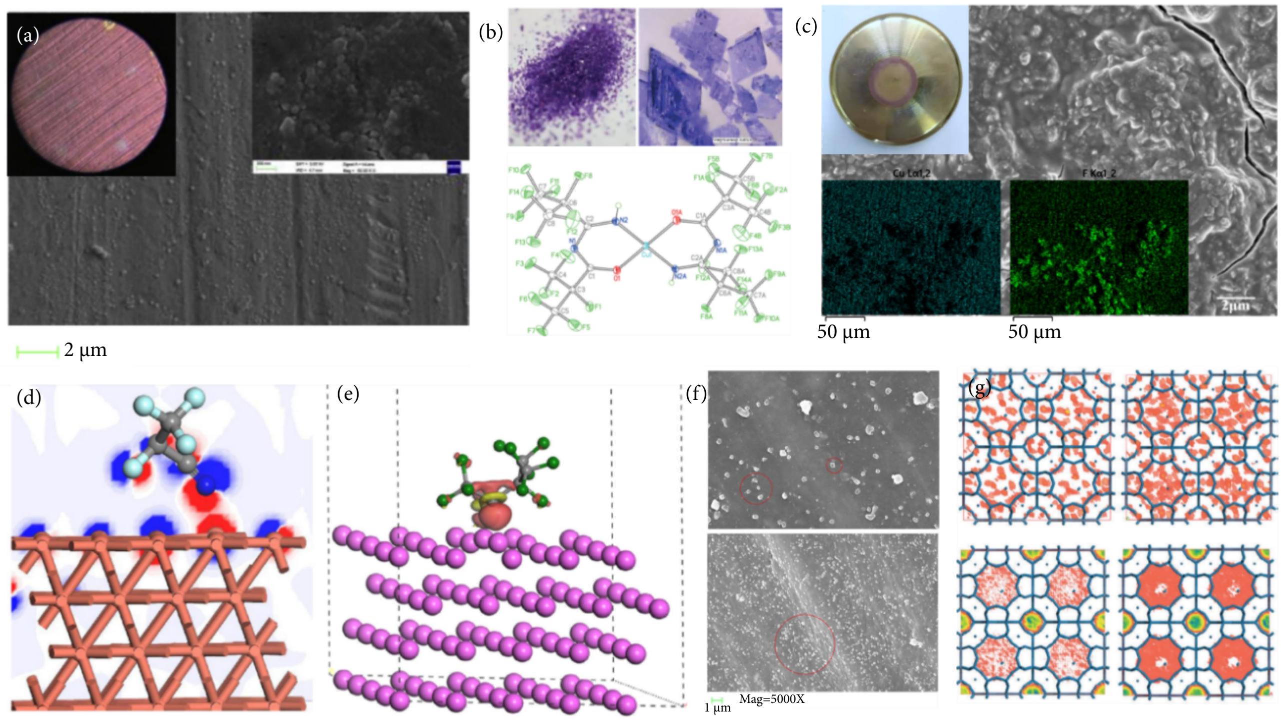

Fig. 10 The materials compatibility of eco-friendly insulating gas. **(a)** The morphology of copper after interacted with C_4F_7N at 220°C for 40 h. Reprinted with permission from Ref. [202], © 2019 Elsevier Ltd. **(b)** Microscope photograph of violet crystals and molecular structure of square planar copper(II) complex. Reprinted with permission from Ref. [206], © 2020 WILEY-VCH Verlag GmbH & Co. KGaA, Weinheim. **(c)** The morphology of copper electrode after 96 h PD (15% C_4F_7N/CO_2 gas mixture, 0.15 MPa) Reprinted with permission from Ref. [206], © 2020 WILEY-VCH Verlag GmbH & Co. KGaA, Weinheim. **(d)** The electron density difference of C_4F_7N-Cu(1 1 1) interface. Reprinted with permission from Ref. [207], © 2018 Elsevier Ltd. **(e)** The electron density difference of $C_5F_{10}O$-Cu(1 1 1) interface. Reprinted with permission from Ref. [208], © 2019 Elsevier Ltd. **(f)** The morgrophy of EPDM after interacted with C_4F_7N/CO_2. Reprinted with permission from Ref. [213], © 2021 Author(s). **(g)** The density fields of HF(up) and CO(down) in the Na-4A zeolite under the pressures of 0.01, 1 kPa. Reprinted with permission from Ref. [218], © 2020 Author(s).

Elastomer

Elastomer or rubber ring plays an important role in GIE considering the relatively high working pressure. At present, assessment on the compatibility between fluorinated-nitrile, ketone with ethylene propylene diene monomer (EPDM), nitrile butadiene rubber (NBR), fluoro rubber has confirmed the incompatibility of EPDM and NBR[210–212]. Specifically, the C_4F_7N-EPDM interaction induced the generation of CO, C_3F_6, C_2H_4, C_2H_6, the crystal precipitation and mechanical degradation of rubber (Figure 10(f))[210]. Moreover, the ethylidene norbornene (ENB)-EPDM demonstrated superior gas-solid stability compared to the dicyclopentadiene (DCPD-EPDM), and the silicone grease coating could further prevent the interaction[211]. Similar studies on the NBR and C_4F_7N confirmed the mechanical properties deterioration with 10.15% decrease of elongation at break and 37% loss of tensile strength[212].

In addition, the sealing performance of buffer gas with a smaller molecular structure should be considered. For example, butyl rubber is tight to CO_2, air, or N_2, while the unsaturated double bonds in the isoprene chain might be oxidized by the discharge induced O_3. The utilization of halogenated butyl rubber (CIIR-BIIR) with a similar molecular structure is recommended. Relevant gas permeability tests confirmed CIIR-BIIR demonstrated a lower permeation rate coefficient than that of EPDM[56]. Further explanations on the design of special sealing rubber for eco-friendly insulating gas are necessary.

Adsorbent

Adsorbent or desiccant is mainly utilized for impurities adsorption especially trace moisture in SF_6-based GIE. For eco-friendly insulating gas, the additional capabilities such as the elimination of toxic and corrosive products is should be considered as the "cumulative effect" of decomposition by-products. Evaluation of the compatibility of γ-Al_2O_3, molecular sieve (3A–5A) found that there existed strong interaction between γ-Al_2O_3 and C_4F_7N, causing consumption of the main insulating gas[213–215].

As for the by-products, it was found that molecular sieves demonstrated a weak adsorption effect on PFCs (CF_4, C_2F_6, C_3F_8) and CO. The 3A–5A molecular sieve is capable of removing C_2N_2, CF_3CN[215]. The microscopic parameters including adsorption isotherm, saturated adsorption capacity, free energy, diffusion coefficient, etc. of gas-adsorbent system were also calculated based on MD, and the superior adsorption performance of HF, COF_2, C_2N_2, CF_3CN, C_2F_5CN was confirmed (Figure 10(g))[216]. The design and synthesis of new adsorbent is highly recommended for the eco-friendly GIE application[217]. The metal organic frameworks (MOFs) with periodic network structures formed by molecular self-assembly of metal ions or ion clusters and organic ligands is a promising selection.

3.5 Biosafety

Biosafety is another significant parameter for eco-friendly insulating gas considering the inevitable exposure of maintenance personnel. Some toxicity properties such as acute toxicity, target organ toxicity have been investigated currently.

LC50

The Material Safety Data Sheet (MSDS) of C_4F_7N and $C_5F_{10}O$

given by 3M indicated that the median lethal concentration (LC50, 4 h, rat) of C_4F_7N, C_4F_7N was 10,000–15,000 μL·L^{-1} (ppm), 14, 000–20,000 μL·L^{-1}, respectively (Figure 11(a)), and the no observed adverse effect level (NOAEL) of 28 days subacute inhalation of C_4F_7N in rats was 500 μL·L^{-1}. The LC50 (4 h, mice) of C_4F_7N given by Wuhan University was 1175 μL·L^{-1} (male) and 1,380 μL·L^{-1} (female), the result given by Schneider was 1600 μL·L^{-1}, the difference in LC50 values was due to the difference in species and weight of the mice used[218,219]. The occupational exposure limits (OEL) of C_4F_7N and $C_5F_{10}O$ were set to 65 μL·L^{-1} and 225 μL·L^{-1}, which is lower than 1000 μL·L^{-1} of SF_6)[218,219]. For the C_4F_7N/CO_2 gas mixture, the LC50 (rat, 4 h) of 4% C_4F_7N-96% CO_2 and 10% C_4F_7N-90% CO_2 gas mixture reaches 16%–21.1% and 9.55%–10%[56]. Considering the content of C_4F_7N in the gas mixture is generally in the range of 4%–10%, the C_4F_7N gas mixture is classified as non-toxic substance according to EU 1272/2008 CLP and Globally Harmonized System (GHS) regulation[56].

At present, the acute toxicity of C_4F_7N or $C_5F_{10}O$ has been preliminarily confirmed to be higher than SF_6 and other eco-friendly gases such as HFO-1234ze(E). There is a lack of in-depth understanding of the inhalation toxicity of C_4F_7N or $C_5F_{10}O$, especially the hazard mechanism to individual vital signs under different exposure cycles (acute, subacute, and chronic).

Target organ toxicity

The preliminary study on the vital signs changing and target organ toxicity of C_4F_7N found that rats or mice would suffer from gloomy spirit, action retardation and abnormal blood cell count after exposure (Figure 11(b)). The pathological tissue slice further confirmed the lung, kidney, intestine and brain injury when the exposure content reaches 1.5%, as shown in Figure 11(c)[220,221]. Besides, the behavioral experiments (spontaneous alternation in the Y-maze and object recognition) on mice that were exposed to 800 μL·L^{-1} and 1500 μL·L^{-1} C_4F_7N indicated the general impact on mobility, anxiety, spatial working memory and recognition memory. The behavioral impairments occurred on day 1, day 7 and object recognition on day 14. The histology and immunohistochemistry tests of the brain further observed histological alterations of pyramidal neuronal layer in the hippocampus, neuroinflammatory astroglial reaction, and microglial alterations[222]. As illustrated in Figure 11(d), C_4F_7N could result in a significant increase in γ-H2Ax/H2Ax levels ratio, and cell loss in the hippocampus, triggering proapoptotic signals including apoptosis, DNA breaks. The gas exposure also causes cellular impact, inducing neuroinflammation and microglia damage.

Considering the potential lung, kidney and brain injury caused by C_4F_7N, the biochemical specific indicators, safety concentration threshold of short-term and long-term exposure should be determined. The utilization of effective personal protective equipment (PPE) is necessary for risk-exposed personnel (Figure 11(e)). Further exploration of reproductive, genetic toxicity of C_4F_7N and other eco-friendly insulating gas should be conducted to guide safety application.

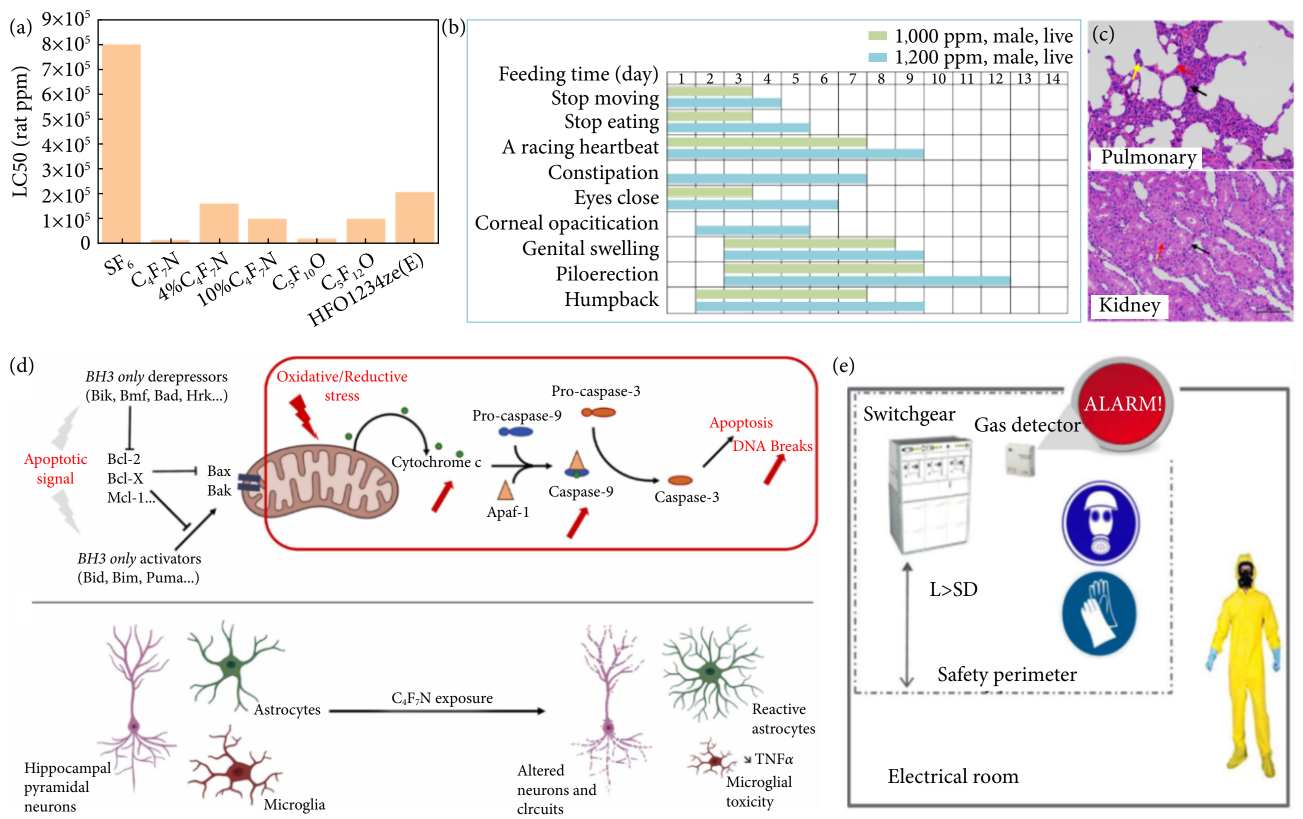

Fig. 11 The biosafety of eco-friendly insulating gas. (a) The LC50 (rat, 4 h) of SF_6 and various eco-friendly insulating gas. **(b)** The changes in vital signs of mice that survived exposure to different concentrations of the gas over a 14-day observation period. Reprinted with permission from Ref. [223], © 2020 Taylor & Francis. **(c)** Pathological section of the pulmonary and kidney after 2% C_4F_7N exposure for 4 h. Reprinted with permission from Ref. [222], © 2019 Elsevier Ltd. **(d)** Summary of the toxicity observed in the mice brains after exposure to C_4F_7N (up) and the impact on brain cells (down). Reprinted with permission from Ref. [224], © 2022 Elsevier Ltd. **(e)** Representation of an electrical room with a safety perimeter around the electrical switchgear when gas leakage is detected. Reprinted with permission from Ref. [232], © 2018 Author(s).

By-products toxicity

The generation of various toxic by-products is inevitable for GIE, especially for arc-quenching or under fault conditions. The highly toxic H_2S, SO_2, SOF_2, HF, SO_2F_2 is found in SF_6 GIE. For eco-friendly insulating gas such as C_4F_7N, the 100 times breaking tests on the 145 kV circuit breaker with 6% C_4F_7N-89.1% CO_2-4.9% O_2 under 40 kA short circuit current possessed the acute inhalation toxicity (LC50) of 3.8%, lower than 7.4% of SF_6[223]. The 200 times breaking tests on the load switch filled with 57% C_4F_7N-43% air at 630 A resulted in the LC50 of 31 μL·L^{-1} (male mice) and 34 μL·L^{-1} (female mice), respectively. The most toxic by-product was perfluoroisobutylene (C_4F_8) with the LC50 of 0.5 μL·L^{-1}, followed by C_2N_2(175 μL·L^{-1}), COF_2 (180 μL·L^{-1}), CF_3CN (250 μL·L^{-1}), and CO (1,880 μL·L^{-1})[224]. In addition, the 42% $C_5F_{10}O$-58% Air gas mixture after 100 breakings at 630 A demonstrated the LC50 of 21,000 μL·L^{-1}, which was much higher than SF_6 under the same conditions[225].

Overall, the acute inhalation toxicity of the gas mixture after arc-quenching significantly changed due to the formation of various toxic by-products, which is determined by the content of main insulating gas, number of operations and breaking capacity. There are few studies on the biosafety of eco-friendly insulating gas under the long-term operation of POF, PD fault conditions. The development of a selective adsorbent or desiccant that can filter out highly toxic decomposition by-products to further improve the application safety of eco-friendly insulating gas-based GIE is urgent.

4 Application of eco-friendly insulating gas

4.1 Medium voltage equipment

MV-GIE is widely used in an urban distribution network such as building, subway, airport. At present, several kinds of eco-friendly MV-GIE have been developed. The first $C_5F_{10}O$/air based ring main units (RMU) was proposed by ABB in 2015 (Figure 12(a))[226], which was installed as compact secondary substations (CSS) in the Netherlands and long-term field experience was obtained. The 10.7 kPa $C_5F_{10}O$/129.3 kPa air gas mixture achieved a service voltage of 20 kV and loads up to 630 A. The gas temperature and absolute pressure remained stable during operation, as shown in Figure 12(b). The gas composition analysis showed that heptafluoropropane (C_3F_7H) was the main decomposition by-product (lower than 50 μL·L^{-1}) during the first year. The other 24 kV/630 A MV-GIS was also developed with a minimal operating temperature of −15°C. The gas sample taken from the CB that has done 100 switching operations at around 200 A had no measurable reduction of $C_5F_{10}O$ and the by-products of C_3F_7H (~100 μL·L^{-1}), CF_4, C_3F_6 were generated (Figure 12(c)). The $C_6F_{12}O/CO_2$ based 10 kV C-GIS was also proposed[58, 95, 227].

The C_4F_7N/CO_2 based 12 kV RMU with metal plate to extinguish arc was also designed by China Electric Power Research Institute, as shown in Figure 12(d). The RMU passed the withstand voltage test of 1.2 times the rated insulation level and the active load current opening and closing tests of 630 A for 10 times and of 1000 A for 2 twice[228]. The arc in C_4F_7N/CO_2 demonstrated a lower voltage, wider arc channel and more liable to fall from the metal plate compared to that of SF_6. The flat plate with an insulation cover and CuW static, moving contact was used to improve the switching performance and anti-ablation ability. Besides, the 10 kV/630 kVA GIT with C_4F_7N/CO_2 as the insulating and heat dissipation medium was developed (Figure 12(e))[228]. The average temperature rise of C_4F_7N/CO_2 is higher than that of SF_6 under the same load condition, and the internal heat dissipation structure was optimized.

Besides, the remaining uncertainties regarding the toxicity urge a preferable solution that uses natural gas or proven safe gas, such as air for dielectric medium combined with vacuum technology for current interruption in MV-GIE. Vacuum breaking is a well-known technology used for decades in MV. The moderate pressure increase of air enables SF_6 insulation performance and keeps the same dimensions of switchgear. Other F-gases ($C_5F_{10}O$ or C_4F_7N)

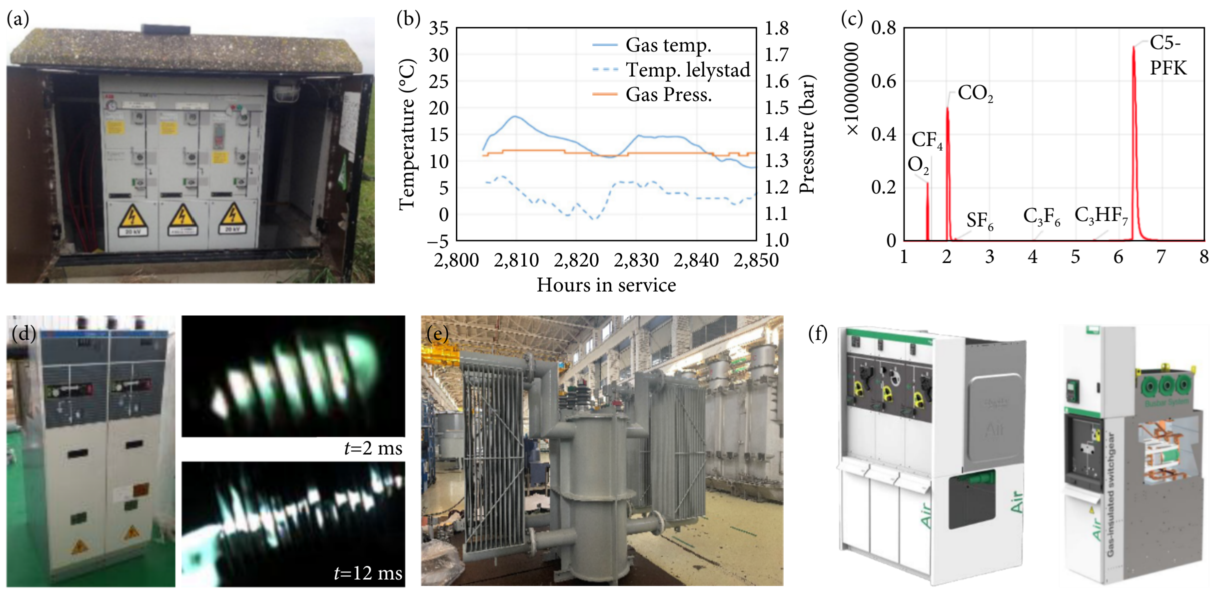

Fig. 12 The design and application of eco-friendly insulating gas based MV-GIE. (a) Air-plus switchgear installed in the Netherlands. Reprinted with permission from Ref. [228], © 2017 IEEE. **(b)** Gas temperature (blue) and absolute pressure (orange) versus time recorded 2800–2850 h for the Air-plus switchgear. Reprinted with permission from Ref. [228], © 2017 IEEE. **(c)** Gas sample is taken from a circuit breaker that has done around 100 switching operations at around 200 A. Source: Johannes Hengstler, Maik Hyrenbach, ABB, in CIGRE WG B3.45 Meeting. **(d)** The 12 kV C_4F_7N/CO_2 Ring Main Unit. Source: Z. Li, China Electric Power Research Institute. **(e)** The 10 kV C_4F_7N/CO_2 GIT. **(f)** The SF_6-free load break switch with shunt vacuum interruption (SVI) technology. Source: C. Preve, Schneider Electric.

with lower GWP than SF_6 have safety concerns, especially for MV switchgear that is close to the public. A gas container with safety concerns cannot be acceptable. The potential carcinogenic, reprotoxic and neurotoxic risks are not known. Moreover, these gases are per- & polyfluoroalkyl substances (PFAS). These substances are currently under the scope of Registration, Evaluation, Authorization and Restriction of Chemicals (REACH regulation of Europe) which is looking to ban all "non-essential" use. As natural alternatives such air exist, fluorocarbons may be banned in the future. Recently, Schneider Electric proposed the innovative SF_6-free load break switch with shunt vacuum interruption (SVI) technology that is set in an epoxy tank (AIS) or stainless-steel tank (GIS)[229,230]. The designed 12–24 kV/630 A load break switches (LBS) keep the same operating mode as the traditional 3-position switch and have been energized in Sweden, France, China in 2019 (Figure 12(f)).

4.2 High voltage equipment

The eco-friendly insulating gas based HV-GIE is also designed and applied since 2015. Specifically, GE launched the world's first C_4F_7N/CO_2 based 145 kV GIS with an inflation pressure of 0.85 MPa, an operating temperature of −25–40°C, and a rated current of 3150 A/40 kA (Figure 13(a))[231]. The device passed the temperature rise and insulation tests required in IEC 62271-203 standard, as well as the terminal fault (TF), short line fault (SLF, L75, and L90) and capacitor breaking test involving CBs. As the mass density of C_4F_7N gas mixture is lower than SF_6, the gas blowing speed and pressure construction are affected during no-load operation and high current arc extinction. Therefore, the chamber volume, channel diameter, and spring of CB unit were optimized. In addition, the EPDM seal ring was also replaced and a new density meter, and pressure relief device were designed and installed. The temperature rise of the conductors given in Figure 13(b) confirmed the addition of a small portion C_4F_7N demonstrates a positive effect on the overall heat dissipation performance. In 2017, the first 145 kV/40 kA equipment was installed in Etzel substation in Switzerland, and operated at 123 kV at the initial stage[232]. In 2018, the same type of GIS was applied in Grimmer substation in France with an operation voltage of 72.5 kV. The maintenance strategy follows SF_6 related regulations and the gas mixing ratio was detected. The second generation C_4F_7N based 145 kV/ 40 kA GIS utilized O_2 as the second additive gas to enhance the switching

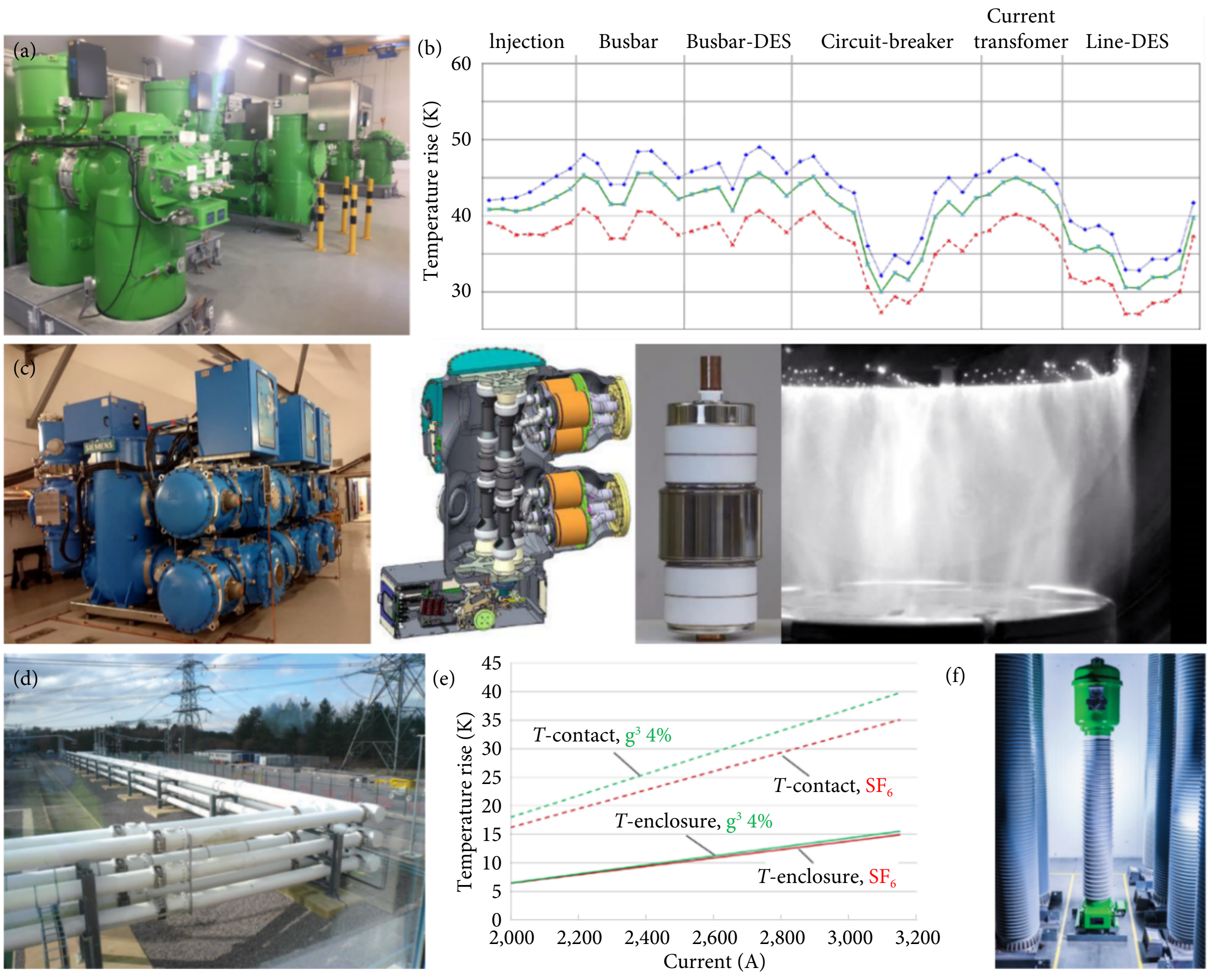

Fig. 13 The design and application of eco-friendly insulating gas based HV-GIE. (a) The 145 kV $C_4F_7N/CO_2/O_2$ based GIS developed by GE. Source: M. Inversin, D. Signing Tsamo, RTE. **(b)** Temperature rise profile along the fully equipped 145 kV GIS bay at 2500 A. (Red) SF_6; (Green) 6% C_4F_7N/94% CO_2 gas mixture; (Blue) CO_2. Source: D. Gautschi, GE Grid Solutions. **(c)** The 145 kV GIS developed by Siemens with 80%N_2/20%O_2 and vacuum interrupter(left). The vacuum interrupter with a height of 0.65 m and a diameter of 0.23 m (middle). The right shows the diffuse stable axial magnetic field (AMF) vacuum arc at 50 kA. Source: K. Kim, ILJIN Electric. **(d)** The 420 kV C_4F_7N/CO_2 GIL developed by GE. Reprinted with permission from Ref. [97], © 2016 IEEE. **(e)** The comparison of temperature rise between C_4F_7N/CO_2 and SF_6. Source: D. Gautschi, GE Grid Solutions. **(f)** The 245 kV C_4F_7N/CO_2 GT developed by GE. Reprinted with permission from Ref. [97], © 2016 IEEE.

performance as O_2 is capable of limiting the generation of gaseous and solid by-products[233]. Besides, the HV GIS with 6% $C_5F_{10}O$/82% CO_2/12% O_2 was also designed for 170 kV/40 kA scene with a working temperature of 5–40°C[234].

The fluoride-free strategy is another solution for eco-friendly GIS, that is, using air insulation associated with vacuum breaking or CO_2 for insulation and breaking with pressure increase compared to SF_6. For example, the world's first 145 kV/40 kA and 170 kV/50 kA GIS with clean air (80% N_2/20% O_2) and vacuum interrupter was developed by Siemens Energy, as shown in Figure 13(c)[235,236]. The contact geometry of CB was realized with the axial magnetic field (AMF) to ensure sufficient arc stability, strength, and suitable spatial distribution. The measured X-rays of the vacuum interrupter were far below the required thresholds of IEC and ANSI/IEEE standards. The first substation was installed and commissioned in 2019 in Norway. Besides, the design of single vacuum-interrupter units up to 245 kV and 63 kA is ongoing currently. The advances in vacuum switching technology will bring promising application for higher voltage fluoride-free GIS.

As for the other HV GIE such as GIL, GE developed the first C_4F_7N/CO_2 420 kV GIL in 2016 with a working pressure of 1.06 MPa and operating temperature of −25–40°C (Figure 13(d))[96]. The equipment passed the lightning impulse, switching impulse and power frequency withstand voltage (PFWV) tests according to IEC 62271-203. The temperature rise on the enclosures with 4% C_4F_7N/96% CO_2 is similar to SF_6, and the contact condition in the range of 2000–4000 A has been fully validated below the corresponding limits (Figure 13(e)). The first 420 kV/63 kA GIL was installed in 2016 at the Sellindge substation. In 2020, the world's first 1000 kV GIL was developed by Ping Gao Group, which possessed a standard unit length of 18 m, a PD intensity of less than 3 pC, and an annual leakage rate lower than 0.01%. Besides, GE also proposed the C_4F_7N/CO_2 based 245 kV current transformer (CT) that passed relevant special tests including PFWV, basic impulse level (BIL), PD, capacitance and dielectric factor as specified by IEC 61869 standard.

Overall, the MV and HV eco-friendly GIE developed currently offer similar performance and footprints with that of SF_6. However, the heat dissipation, and current interruption capability of fluorinated gases are inferior owing to the basic physicochemical properties. The utilization of fluorinated eco-friendly gas or fluorine-free gas are the two main strategies for the next-generation SF_6-free GIE, wherein the advanced possess in repeated arc-quenching of fluorinated gas and high capacity vacuum interruption technology is going to bring breakthrough in the field.

4.3 Maintenance related devices

The application of eco-friendly GIE also requires maintenance related devices including gas management, composition analysis and on-site monitoring, which has been developed gradually. As shown in Figure 14(a), the service cart with the gas filling, recovery and reclaim functions has been proposed and qualified by the French Transmission System Operator (TSO) with a filling accuracy less than 0.1%[231]. Frankly, there exists difference in gas detection objects between eco-friendly and traditional SF_6 GIE. As the main insulating gas determines the insulation level, it is necessary to timely and accurately grasp the gas mixture proportion in the equipment during operation. Meanwhile, the detection of typical or harmful decomposition by-products is also significant for eco-friendly GIE operation and fault diagnosis. The corresponding gas detection technology for eco-friendly insulating gas and relevant by-products are also investigated.

Gas absorption spectroscopy has the advantages of feasible equipment integration, high precision, and great reliability, which has promising potential for on-site gas composition analysis application. The ultraviolet, infrared spectral characteristics of eco-friendly insulating gas have been explored. For example, C_4F_7N possesses an obvious absorption spectrum in the ultraviolet spectral band that has great linearity with C_4F_7N content, as shown in Figure 14(b). The detection of C_4F_7N/CO_2 mixing ratio can be achieved with a detection error less than 5%[237]. The fiber-coupled LED gas sensor was developed for concentration measurement of fluorinated ketones. The dual-wavelength scheme was proposed for gas composition analysis in the harsh environment, achieving the $C_5F_{10}O$ detection limit of Δp=12 Pa and relative concentration accuracy of $\Delta c/c \approx \pm 1\%$[238]. Ultraviolet differential optical absorption spectroscopy (UV-DOAS) was also proposed for the quantification of $C_5F_{10}O$, realizing the detection range of 0.1%–7.5%[239]. In view of the possible equipment gas leakage detection, the infrared-based method was proposed. As shown in Figure 14(c), the infrared band of C_4F_7N with higher absorption intensity and better linearity was found in the range of 750–780 cm^{-1}. The utilization of peak area as the eigenvalue brought the detection error less than 3% for 1%–10% C_4F_7N. Further, the stronger infrared absorption band was found in 1240–1290 cm^{-1}, which demonstrated a superior linear relationship with 0–0.2% C_4F_7N and was suitable for leakage detection[240]. Besides, the subtractive spectrum technology combined with long optical path gas cell and FTIR was employed for by-product analysis. The subtractive spectrum given in Figure 14(d) confirmed the rapid analysis of C_3F_6, CO, and COF_2 can be achieved[241]. For the device level, the gas analyzer for mixing ratio, moisture and decomposition by-products detection C_4F_7N has been developed (Figure 14(e))[231]. In another work, the multi-parameter sensor system was designed with a piezoresistive transmitter for pressure detection, a temperature sensor and a digital density meter for density detection. The device provides a measurement uncertainty below ±4%, a resolution better than 1% of the $C_5F_{10}O$ content and has been mounted on GIS for one year[242].

Besides, building a novel power system with extensive interconnection and intelligent interaction features puts forward higher requirements for the intelligent perception of GIE status. Advanced micro-nano sensors with low power consumption and high sensitivity are the basic components. For eco-friendly insulating gas, the room temperature electrochemical sensor was reported recently. As illustrated in Figure 14(f), SnO_2 was found to possess superior sensitivity to C_4F_7N while a relatively high temperature is required for gas desorption[243]. The $Ti_3C_2T_x$-SnO_2 nanocomposite with superior sensing performance was achieved, wherein $Ti_3C_2T_x$ with specific area works as the sensing framework and SnO_2 nanoparticles take the role of bait to attract C_4F_7N molecule. The designed $Ti_3C_2T_x$-SnO_2 gas sensor exhibited an 8.8% response to 45 μL·L^{-1} C_4F_7N within 180 s, which raise the sensitivity by 460% compared to the pristine $Ti_3C_2T_x$ and provides a promising route for gas leakage monitoring[244]. Further, the “Sensgear” concept for comprehensive monitoring of eco-friendly GIE to achieve intelligent equipment was proposed, as shown in Figure 14(g). Specifically, the GPS/GSM antenna, gas density, auxiliary/limit switch, cabinet temperature, ambient temperature sensors are embedded into the GIE during design and assemble, and relevant detected data will be collected and submitted through the Internet of Things (IoT) connectivity device. The realization of this concept will bring revolutionary progress to the SF_6-free GIE in the power industry.

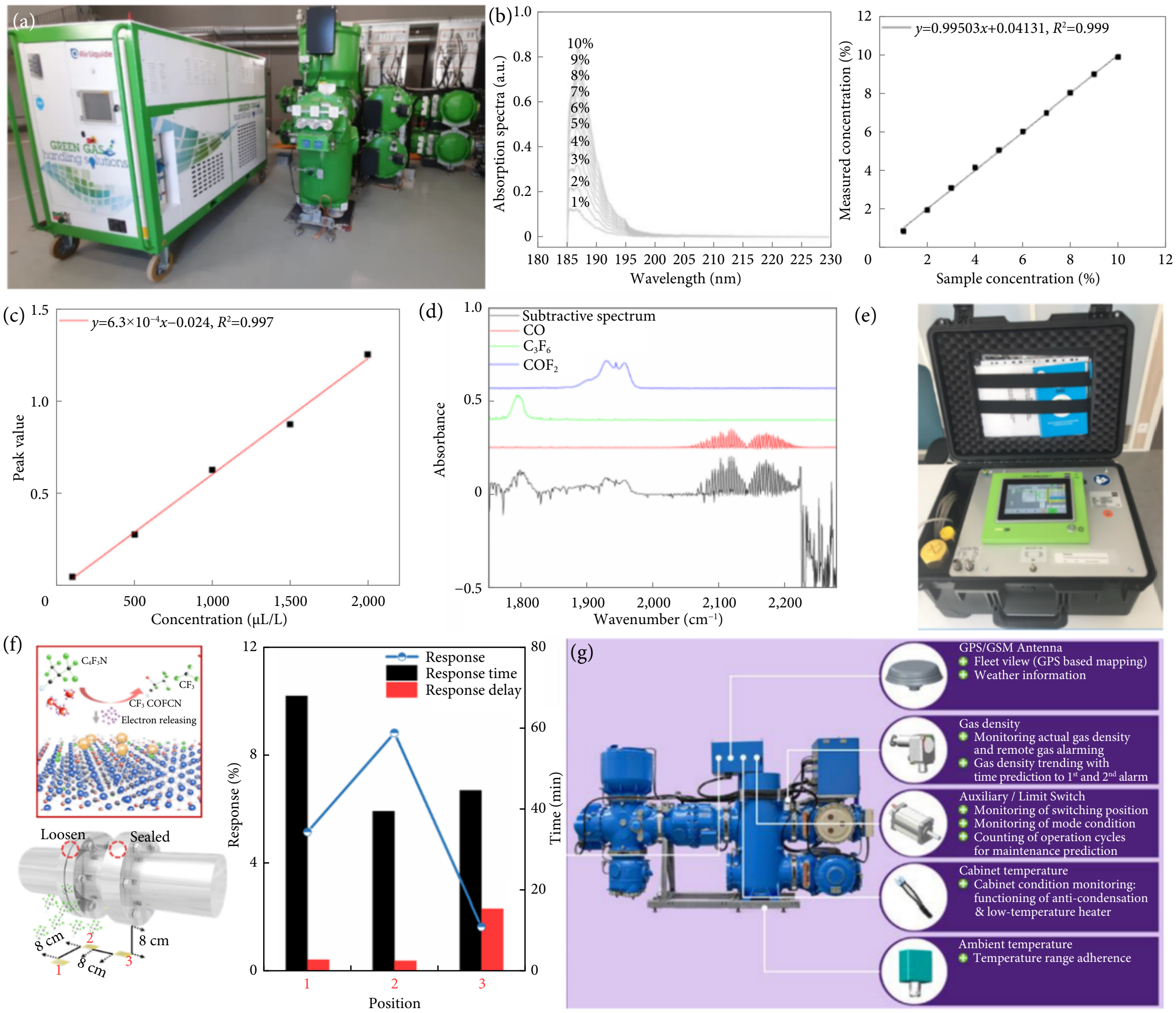

Fig. 14 The design and application of maintenance related devices for eco-friendly insulating gas based GIE. (a) The gas handling equipment for C_4F_7N based GIE. Source: M. Inversin, D. Signing Tsamo, RTE. **(b)** The ultraviolet spectral absorption spectrum of the C_4F_7N/CO_2 gas mixture with different content of C_4F_7N(left) and the obtained concentration inversion curves. Reprinted with permission from Ref. [239], © 2019 Author(s). **(c)** The infrared spectroscopy fitting curve of C_4F_7N/CO_2 gas mixture with different content of C_4F_7N. Reprinted with permission from Ref. [242], © 2019 Elsevier Ltd. **(d)** The infrared spectroscopy of the C_4F_7N decomposition by-product C_3F_6, CO and COF_2. Reprinted with permission from Ref. [243], © 2020 Elsevier Ltd. **(e)** The C_4F_7N gas mixture analyzer used on site. Source: M. Inversin, D. Signing Tsamo, RTE. **(f)** The $SnO_2/Ti_3C_2T_x$ gas sensor for C_4F_7N leakage detection. Reprinted with permission from Ref. [245], © 2022 American Chemical Society. **(g)** Overview of the Sensgear concept and measurement quantities. Source: M. Kuschel, Siemens Energy.

5 Challenges and perspectives

Nowadays, the increasing policy restrictions and climate control measures of SF_6 further promote the development and application of eco-friendly insulating gas. Although substantial efforts have been made in the field, several significant challenges remain that call for more solutions to achieve the next-generation SF_6-free GIE in the future.

5.1 Challenges

Stability

The low GWP essentially reflects inferior stability, while electrical stability is highly pursued by GIE. The existing "cumulative effect" of decomposition by-products and continuous consumption of eco-friendly electron affinity gas under discharge needs to be addressed. The strategies that can hinder the critical reaction pathways of gas decomposition and product generation should be clarified. For example, the design of other "decomposition inhibition" or "by-product regulation" additive gas and optimization of operation conditions (gas pressure, mixing ratio) to improve the stability is necessary. The clarification of the limit content of various impurities in the gas mixture should also be conducted.

Interruption

The study on arc-quenching characteristics is significantly less extensive than that on dielectric properties. Existing research has confirmed that eco-friendly insulating gas has the load current interruption capability, while there exist challenges such as the decline of dielectric strength, and precipitation of solid by-products. Most eco-friendly gases cannot recombine into themselves after dissociation during arc extinction. This requires us to pay more attention to the arc-quenching performance of eco-friendly gases. However, some basic data, such as electron-impact cross-sections and spectrum data, are still unavailable and require more investigation. The departure from thermodynamic and chemical equilibrium in the current zero of arc extinction also brings us great difficulties in arc modeling. Further optimization on the eco-friendly arc extinguishing composition and the structure of the CB, utilization of auxiliary arc extinguishing means, etc. to improve the interruption capacity and inhibit the solid by-product precipitation is significant to realize the reliable application in arc extinguishing scenarios.

Compatibility

Most eco-friendly insulating gases demonstrate great compatibility with aluminum, silver, while fluorinated-nitrile, ketones with active functional groups are incompatible with copper. This also exists for functional materials such as sealing rubber, adsorbent. The role of solid surface in the decomposition of eco-friendly insulating gas needs to be clarified, and alternative solutions or anti-corrosion strategies should be sought for incompatible materials. For example, grain boundary engineering, fluorinated coating might be useful. Besides, the highly selective adsorbent that is used for toxic, corrosive by-product elimination should be designed for specific eco-friendly insulating gas. Further investigations on the impact of additives (oxygen, etc.), and impurities on materials compatibility should be conducted.

Health and safety

Carcinogenic, mutagenic and reprotoxic (CMR) effects, bone marrow cytotoxic effects (cytotoxicity involves the death of cells), and neurotoxic effects of the new gas candidates must be well known in order to define the personal protection of operators and users and to insure the safety of people who could be in contact with these gases in case of accidental leakage.

Maintenance

The MV eco-friendly GIE has achieved small-scale application in China and various HV realized test running in the EU, etc. The operation and maintenance strategy mainly refers to the SF_6 GIE currently, and few standards on SF_6-free GIE are proposed. The safety protection measures for eco-friendly gas and decompaction by-products with toxicity should be clarified. The monitoring of mixing ratio, gas pressure, solid precipitation, etc. is recommended for fluorocarbon based GIE to ensure long-term operation reliability. Besides, the principle for sub-package, disposal and recovery of eco-friendly insulating gas should be provided.

5.2 Perspectives

SF_6 control and recycling

Frankly, SF_6 outperforms various eco-friendly insulating gas currently in terms of stability, self-recovery, and current interruption. It is urgent to establish and improve the whole cycle tracking and supervision of SF_6, and strictly prohibit random emission, to avoid the climate impact caused by SF_6 considering the large number of service equipment. Meanwhile, strengthening the recovery, purification, and reuse of SF_6 or SF_6/N_2 to improve the reuse rate and service life of existing SF_6 will be a short-term trend. For the SF_6 waste gas that has no recycling value, the development of harmless degradation and treatment strategy to achieve in-situ disposal will be developed.

Insulation coordination

There exists a tradeoff between dielectric strength and liquefaction temperature of eco-friendly insulating gas, and the high sensitivity to electric field inhomogeneity also exists. Optimization of insulation design or coordination based on gas properties will further enhance the operating reliability. For example, gas-solid composite insulation design, and surface/space charge suppression needs to be further explored. The improvement of key materials processing technology to avoid latent defects is also significant.

Arc-quenching mechanism

It is anticipated that the arc-quenching characteristics of eco-friendly gases will be investigated comprehensively by numerical and experimental approaches. The works on the basic data including particle compositions, thermodynamic properties, transport coefficients, radiation coefficients, and dielectric breakdown properties, will be gradually improved, with the development of new techniques, e.g. quantum chemistry and artificial intelligence. To deeper and better understand the arc interruption of eco-friendly gases, the 3-D MHD models instead of 1-D and 2-D should be developed, and more sophisticated models, such as radiative energy transport, nozzle ablation, contact erosion, turbulence, and the departure from equilibrium, should be coupled.

Scientific management of PFAS

In 2022, 3M decided to exit PFAS manufacturing by the end of 2025. Totally 58 kinds of fluoropolymers, fluorinated fluids, and PFAS-based additive products are affected, including C_4F_7N, $C_5F_{10}O$[245]. PFAS are critical in several fields such as semiconductors, batteries, refrigerants, airplanes, medical technologies, etc. This decision does not mean to deny the application potential of fluorinated nitrile and ketones, while the impact on application of SF_6-free GIE needs to be assessed. The natural gas combined with the vacuum circuit breaker possesses technical bottlenecks in EHV and UHV application. The scientific, reasonable application and management of PFAS are appealed.

Development of new gas

The development of computational chemistry provides effective tools for new gas design, especially the clarification of the structure-activity relationship between gas molecules and insulation properties, environmental features, toxicity, etc. Besides, the synthesis of designed molecules also requires interdisciplinary cooperation including chemical engineering, physics, and biomedical science. The further trend is to develop non-PFAS eco-friendly insulating gas with advanced comprehensive performance.

Intelligent SF_6-free equipment

The “novel power system” requires higher operational reliability and information perception ability of various equipment including GIE. The status assessment of eco-friendly insulating gas is also significant. The development of advanced sensing technologies and distributed devices for SF_6-free GIE brings promising application reliability improvement. Meanwhile, the new gas composition sensor, discharge monitoring, and pressure detector are expected to be embedded with the equipment.

6 Conclusion

In this paper, we systematically summarized recent advances in eco-friendly insulating gas and the development of SF_6-free GIE. The increasing SF_6 emission in the world urged substitutes with advanced features in dielectric insulation, arc-quenching, stability, material compatibility as well as bio-safety. The in-detail process of the design and assessment of various eco-friendly insulating gases was highlighted, and representative applications were provided. We also summarized the existing challenges and future development trends in the field, which hopefully steer the development of eco-friendly insulating gas and GIE.

Acknowledgements

This work was supported in part by the National Natural Science Foundation of China (Nos. 52277144, 52107145, and 51907023) and the fellowship of China Postdoctoral Science Foundation (No. 2022M712446).

Article history

Received: 16 December 2022; Revised: 5 January 2023; Accepted: 15 January 2023

Additional information

Declaration of competing interest

The authors have no competing interests to declare that are relevant to the content of this article.

References

[1] Zeng, F. P., Wu, S. Y., Lei, Z. C., Li, C., Tang, J., Yao, Q., Miao, Y. L. (2020). SF_6 fault decomposition feature component extraction and triangle fault diagnosis method. *IEEE Transactions on Dielectrics and Electrical Insulation*, 27: 581–589.

[2] Ryan, H. M., Lightle, D., Milne, D. (1985). Factors influencing dielectric performance of SF_6 insulated GIS. *IEEE Transactions on Power Apparatus and Systems*, PAS-104: 1526–1535.

[3] Hu, L., Ottinger, D., Bogle, S., Montzka, S., DeCola, P., Dlugokencky, E., Andrews, A., Thoning, K., Sweeney, C., Dutton, G., et al. (2022). Declining, seasonal-varying emissions of sulfur hexafluoride from the United States point to a new mitigation opportunity. Available at: https://doi.org/10.5194/egusphere-2022-862, 2022.

[4] Ahmad Raza, T., Kamran, M., Khallidoon, M. U., Akhtar, M. N. (2022). Potential of eco-friendly gases to substitute SF_6 for electrical HV applications as insulating medium: A review. *Turkish Journal of Electrical Power and Energy Systems*, 2: 94–102.

[5] Dervos, C. T., Vassiliou, P. (2000). Sulfur hexafluoride (SF_6): Global environmental effects and toxic byproduct formation. *Journal of the Air & Waste Management Association*, 50: 137–141.

[6] Fang, X. K., Hu, X., Janssens-Maenhout, G., Wu, J., Han, J. R., Su, S. S., Zhang, J. B., Hu, J. X. (2013). Sulfur hexafluoride (SF_6) emission estimates for China: An inventory for 1990–2010 and a projection to 2020. *Environmental Science & Technology*, 47: 3848–3855.

[7] Global Monitoring Laboratory Earth System Research Laboratories. (2022). Sulfur hexafluoride (SF_6) - Combined Dataset Available at: https://www.esrl.noaa.gov/gmd/hats/combined/SF6.html.

[8] Zhou, S., Teng, F., Tong, Q. (2018). Mitigating sulfur hexafluoride (SF_6) emission from electrical equipment in China. *Sustainability*, 10: 2402.

[9] Devins, J. C. (1980). Replacement gases for SF_6. *IEEE Transactions on Electrical Insulation*, EI-15: 81–86.

[10] Rabie, M., Franck, C. M. (2018). Assessment of eco-friendly gases for electrical insulation to replace the most potent industrial greenhouse gas SF_6. *Environmental Science & Technology*, 52: 369–380.

[11] Franck, C. M., Chachereau, A., Pachin, J. (2021). SF_6-free gas-insulated switchgear: Current status and future trends. *IEEE Electrical Insulation Magazine*, 37: 7–16.

[12] Beroual, A., Haddad, A. M. (2017). Recent advances in the quest for a new insulation gas with a low impact on the environment to replace sulfur hexafluoride (SF_6) gas in high-voltage power network applications. *Energies*, 10: 1216.

[13] Zhang, B. Y., Xiong, J. Y., Chen, L., Li, X. W., Murphy, A. B. (2020). Fundamental physicochemical properties of SF_6-alternative gases: A review of recent progress. *Journal of Physics D: Applied Physics*, 53: 173001.

[14] Li, X. W., Zhao, H., Murphy, A. B. (2018). SF_6-alternative gases for application in gas-insulated switchgear. *Journal of Physics D: Applied Physics*, 51: 153001.

[15] Xiao, S., Shi, S. Y., Li, Y., Ye, F. C., Li, Y. L., Tian, S. S., Tang, J., Zhang, X. X. (2021). Review on decomposition characteristics of eco-friendly gas insulating medium for high voltage gas insulated equipment. *Journal of Physics D: Applied Physics*, 54: 373002.

[16] Yang, Y., Gao, K. L., Ding, L. J., Bi, J. G., Yuan, S., Yan, X. L. (2021). Review of the decomposition characteristics of eco-friendly insulation gas. *High Voltage*, 6: 733–749.

[17] Pan, B. F., Wang, G. M., Shi, H. M., Shen, J. H., Ji, H. K., Kil, G. S. (2020). Green gas for grid as an eco-friendly alternative insulation gas to SF_6: A review. *Applied Sciences*, 10: 2526.

[18] Owens, J., Xiao, A., Bonk, J., DeLorme, M., Zhang, A. (2021). Recent development of two alternative gases to SF_6 for high voltage electrical power applications. *Energies*, 14: 5051.

[19] Tu, Y. P., Chen, G., Wang, C., Shao, Y. M., Tong, Y. J., Li, C. Y., Ma, G. M., Shahsavarian, T. (2020). Feasibility of C_3F_7 CN/CO_2 gas mixtures in high-voltage DC GIL: A review on recent advances. *High Voltage*, 5: 377–386.

[20] Chen, G., Tu, Y. P., Wang, C., Wang, J., Yuan, Z. K., Ma, G. M., Wang, J., Qi, B., Li, C. Y. (2019). Environment-friendly insulating gases for HVDC gas-insulated transmission lines. *CSEE Journal of Power and Energy Systems*, 7: 510–529.

[21] Parthiban, A., Gopal, A. A. R., Siwayanan, P., Chew, K. W. (2021). Disposal methods, health effects and emission regulations for sulfur hexafluoride and its by-products. *Journal of Hazardous Materials*, 417: 126107.

[22] Wang, X. H., Gao, Q. Q., Fu, Y. W., Yang, A. J., Rong, M. Z., Wu, Y., Niu, C. P., Murphy, A. B. (2016). Dominant particles and reactions in a two-temperature chemical kinetic model of a decaying SF_6 arc. *Journal of Physics D: Applied Physics*, 49: 105502.

[23] Mahdi, A. S., Abdul-Malek, Z., Arshad, R. N. (2022). SF_6 decomposed component analysis for partial discharge diagnosis in GIS: A review. *IEEE Access*, 10: 27270–27288.

[24] Malik, N. H., Qureshi, A. H. (1979). A review of electrical breakdown in mixtures of SF_6 and other gases. *IEEE Transactions on Electrical Insulation*, EI-14: 1–13.

[25] Maiss, M., Brenninkmeijer, C. A. M. (1998). Atmospheric SF_6: trends, sources, and prospects. *Environmental Science & Technology*, 32: 3077–3086.

[26] Fang, X., Thompson, R. L., Saito, T., Yokouchi, Y., Kim, J., Li, S., Kim, K. R., Park, S., Graziosi, F., Stohl, A. (2014). Sulfur hexafluoride (SF_6) emissions in East Asia determined by inverse modeling. *Atmospheric Chemistry and Physics*, 14: 4779–4791.

[27] Simmonds, P. G., Rigby, M., Manning, A. J., Park, S., Stanley, K. M., McCulloch, A., Henne, S., Graziosi, F., Maione, M., Arduini, J., Reimann, S., Vollmer, M. K., Mühle, J., O'Doherty, S., Young, D., Krummel, P. B., Fraser, P. J., Weiss, R. F., Salameh, P. K., Harth, C. M., Park, M. K., Park, H., Arnold, T., Rennick, C., Steele, L. P., Mitrevski, B., Wang, R. H. J., Prinn, R. G. (2020). The increasing atmospheric burden of the greenhouse gas sulfur hexafluoride (SF_6). *Atmospheric Chemistry and Physics*, 20: 7271–7290.

[28] Rigby, M., Prinn, R. G., O'Doherty, S., Miller, B. R., Ivy, D., Mühle, J., Harth, C. M., Salameh, P. K., Arnold, T., Weiss, R. F., Krummel, P. B., Steele, L. P., Fraser, P. J., Young, D., Simmonds, P. G. (2014). Recent and future trends in synthetic greenhouse gas radiative forcing. *Geophysical Research Letters*, 41: 2623–2630.

[29] United States Environmental Protection Agency. (2022). Inventory of U.S. Greenhouse Gas Emissions and Sinks. https://www.epa.gov/ghgemissions/inventory-us-greenhouse-gas-emissions-and-sinks.

[30] Widger, P., Haddad, A. (2018). Evaluation of SF_6 leakage from gas insulated equipment on electricity networks in great Britain. *Energies*, 11: 2037.

[31] Iwata, H., Okada, K. (2014). Greenhouse gas emissions and the role

of the Kyoto Protocol. *Environmental Economics and Policy Studies*, 16: 325–342.
[32] Johnston, J. (2008). Climate change confusion and the supreme court: The misguided regulation of greenhouse gas emissions under the clean air act. *Notre Dame Law Rev*, 84: 1–74.
[33] EU. Regulation (EU) No 517/2014 of the European Parliament and of the Council of 16 April 2014 on fluorinated greenhouse gases and repealing Regulation (EC) No 842/2006; 2014.
[34] EU. Regulation (EC) No 842/2006 of the European Parliament and of the Council of 17 May 2006 on certain fluorinated greenhouse gases; 2006.
[35] GB/T 28537-2012, The use and handling of SF6 in high-voltage switchgear and controlgear.
[36] GB/T-32151.2-2015, Requirements of the greenhouse gas emissions accounting and reporting. Part 2: Power grid enterprise.
[37] Rotmans, J., Den Elzen, M. G. J. (1992). A model-based approach to the calculation of global warming potentials (GWP). *International Journal of Climatology*, 12: 865–874.
[38] Myhre, G., Stordal, F. (1997). Role of spatial and temporal variations in the computation of radiative forcing and GWP. *Journal of Geophysical Research Atmospheres*, 102: 11181–11200.
[39] Montzka, S. A., Reimann, S., Engel, A., Krüger, K., O'Doherty, S., Sturges, W. T., Blake, D., Dorf, M., Fraser, P., Froidevaux, L. et al. (2011). Ozone-depleting substances (ODSs) and related chemicals (chapter 1). Available at: https://tsapps.nist.gov/publication/get_pdf.cfm?pub_id=909747.
[40] Claxton, T., Hossaini, R., Wild, O., Chipperfield, M. P., Wilson, C. (2019). On the regional and seasonal ozone depletion potential of chlorinated very short-lived substances. *Geophysical Research Letters*, 46: 5489–5498.
[41] Chu, F. Y. (1986). SF_6 decomposition in gas-insulated equipment. *IEEE Transactions on Electrical Insulation*, EI-21: 693–725.
[42] Zeng, F. P., Li, H. T., Cheng, H. T., Tang, J., Liu, Y. L. (2021). SF_6 decomposition and insulation condition monitoring of GIE: A review. *High Voltage*, 6: 955–966.
[43] Kessler F, Sarfert-Gast W, Ise M, et al. (2017). Interaction of low global warming potential gaseous dielectrics with materials of gas-insulated systems, In: Proceedings of the 20th International Symposium High Voltage Engineering, Buenos Aires, Argentina.
[44] Rokunohe, T., Yagihashi, Y., Endo, F., Oomori, T. (2006). Fundamental insulation characteristics of air; N_2, CO_2, N_2/O_2, and SF_6/N_2 mixed gases. *Electrical Engineering in Japan*, 155: 9–17.
[45] Guo, C., Zhang, Q. G., Wen, T. (2016). A method for synergistic effect evaluation of SF_6/N_2 gas mixtures. *IEEE Transactions on Dielectrics and Electrical Insulation*, 23: 211–215.
[46] Zhao, S., Xiao, D. M. (2020). Research progress on synergistic effect between insulation gas mixtures. In Xiao, D. M., Sankaran, K. (Eds.) *Modern Applications of Electrostatics and Dielectrics*. London, UK: IntechOpen.
[47] Deng, Y. K., Xiao, D. M. (2012). Analysis of the insulation characteristics of *c*-C_4F_8 and N_2 gas mixtures by Boltzmann equation method. *The European Physical Journal Applied Physics*, 57: 20801.
[48] Zhao, X. L., Jiao, J. T., Li, B., Xiao, D. M. (2016). The electronegativity analysis of *c*-C_4F_8 as a potential insulation substitute of SF_6. *Plasma Science and Technology*, 18: 292–298.
[49] Takahashi, K., Tachibana, K. (2001). Solid particle production in fluorocarbon plasmas. I. Correlation with polymer film deposition. *Journal of Vacuum Science & Technology A: Vacuum, Surfaces, and Films*, 19: 2055–2060.
[50] Xiao, S., Tian, S. S., Zhang, X. X., Cressault, Y., Tang, J., Deng, Z. T., Li, Y. (2018). The influence of O_2 on decomposition characteristics of *c*-C4F8/N2 environmental friendly insulating gas. *Processes*, 6: 174.
[51] Xiao, S., Zhang, X. X., Tang, J., Liu, S. Q. (2018). A review on SF_6 substitute gases and research status of CF_3I gases. *Energy Reports*, 4: 486–496.
[52] Chen, L. J., Widger, P., Kamarudin, M., Griffiths, H., Haddad, A. (2016). CF_3I gas mixtures: Breakdown characteristics and potential for electrical insulation. *IEEE Transactions on Power Delivery*, 32: 1089–1097.
[53] Widger, P., Haddad, A. (2017). Solid by-products of a CF_3I–CO_2 insulating gas mixtures on electrodes after lightning impulse breakdown. *Journal of Physics Communications*, 1: 025010.
[54] Kamarudin, M. S., Haddad, A., Kok, B. C., Jamail, N. A. M. (2017). Pressurized CF_3I-CO_2 gas mixture under lightning impulse and its solid by-products. *International Journal of Electrical and Computer Engineering*, 7: 3088.
[55] Preve, C., Lahaye, G., Richaud, M., Maladen, R., Penelon, T., Galas, S. (2017). Hazard study of medium-voltage switchgear with SF_6 alternative gas in electrical room. *CIRED - Open Access Proceedings Journal*, 2017: 198–201.
[56] Kieffel, Y. (2016). Characteristics of g3 - an alternative to SF_6. In Proceedings of the 2016 IEEE International Conference on Dielectrics (ICD). Montpellier, France.
[57] Mantilla, J. D., Gariboldi, N., Grob, S., Claessens, M. (2014). Investigation of the insulation performance of a new gas mixture with extremely low GWP. In: Proceedings of the 2014 IEEE Electrical Insulation Conference (EIC). Philadelphia, PA, USA.
[58] Hyrenbach, M., Hintzen, T., Müller, P., Owens, J. (2015). Alternative gas insulation in medium-voltage switchgear. In: Proceedings of the 23rd International Conference on Electricity Distribution, Lyon, France.
[59] Tian, S. S., Zhang, X. X., Xiao, S., Zhang, J., Chen, Q., Li, Y. (2019). Application of $C_6F_{12}O/CO_2$ mixture in 10kV medium-voltage switchgear. *IET Science, Measurement & Technology*, 13: 1225–1230.
[60] Nair, V. (2021). HFO refrigerants: A review of present status and future prospects. *International Journal of Refrigeration*, 122: 156–170.
[61] Rabie, M., Franck, C. M. (2018). Comparison of gases for electrical insulation: Fundamental concepts. *IEEE Transactions on Dielectrics and Electrical Insulation*, 25: 649–656.
[62] Xiao, S., Han, P., Li, Y., Li, Z., Ye, F. C., Li, Y. L., Tang, J., Xia, Y. L., Zhang, X. X. (2021). Insulation performance and electrical field sensitivity properties of HFO-1336mzz(E)/CO_2: A new eco-friendly gas insulating medium. *IEEE Transactions on Dielectrics and Electrical Insulation*, 28: 1938–1948.
[63] Katsuyuki, T. (2016). Measurements of vapor pressure and saturated liquid density for HFO–1234ze(E) and HFO–1234ze(Z). *Journal of Chemical & Engineering Data*, 61: 1645–1648.
[64] Tanaka, K., Ishikawa, J., Kontomaris, K. K. (2017). Thermodynamic properties of HFO-1336mzz(E) (*trans*-1, 1, 1, 4, 4, 4-hexafluoro-2-butene) at saturation conditions. *International Journal of Refrigeration*, 82: 283–287.
[65] Zhang, C. H., Shi, H. X., Cheng, L., Zhao, K., Xie, X. Y., Ma, H. B. (2016). First principles based computational scheme for designing new SF_6 replacements. *IEEE Transactions on Dielectrics and Electrical Insulation*, 23: 2572–2578.
[66] Rabie, M., Dahl, D. A., Donald, S. M. A., Reiher, M., Franck, C. M. (2013). Predictors for gases of high electrical strength. *IEEE Transactions on Dielectrics and Electrical Insulation*, 20: 856–863.
[67] Meurice, N., Sandre, E., Aslanides, A., Vercauteren, D. P. (2004). Simple theoretical estimation of the dielectric strength of gases. *IEEE Transactions on Dielectrics and Electrical Insulation*, 11: 946–948.
[68] Yu, X. J., Hou, H., Wang, B. S. (2018). *A priori* theoretical model for discovery of environmentally sustainable perfluorinated compounds. *The Journal of Physical Chemistry A*, 122: 3462–3469.
[69] Yu, X. J., Hou, H., Wang, B. S. (2017). Prediction on dielectric strength and boiling point of gaseous molecules for replacement of SF_6. *Journal of Computational Chemistry*, 38: 721–729.
[70] Hua, H., Xiaojuan, Y., Wenjun, Z., Yunbai, L., Baoshan, W. (2018). Theoretical investigations on the structure. activity relationship to the dielectric strength of the insulation gases. *Chemical Journal of Chinese Universities*, 39: 2477–2484.

[71] Hua, H., Baoshan, W. (2021). Group additivity theoretical model for the prediction of dielectric strengths of the alternative gases to SF_6. *Chemical Journal of Chinese Universities*, 42: 3709–3715.

[72] Chen, Q., Qiu, R., Lin, L., Cheng, S., Zhang, C. (2019). Selection of potential substitutes for SF_6 based on density functional theory. *High Voltage Engineering*, 45: 1026–1033.

[73] Lin, L., Qingguo, C., Song, C. (2018). The analysis of SF_6 potential alternative gas dielectric strength based on density functional theory (in Chinese). *Transactions of China Electrotechnical Society*, 33: 4382–4388.

[74] Liu, G., Yang, S., Zhang, N., Wang, H., Xiao, J. (2022) Prediction on electrical strength of gaseous medium based on electron location function surface analysis. *High Voltage Engineering*, 48: 2208–2214.

[75] Zhang, N. N., Yang, S., Liu, G. P., Wang, H., Xiao, J. X. (2022). Influence of electron probability density on prediction for insulation strength. *High Voltage Engineering*, 48: 4323–4331.

[76] You, T. P., Dong, X. Z., Zhou, W. J., Zheng, Y., Ren, S. B., Lei, H. Y. (2022). Study on gas molecular structure parameters based on maximum information coefficient. *IEEE Transactions on Dielectrics and Electrical Insulation*, 29: 1633–1639.

[77] Sun, H., Liang, L. Q., Wang, C. L., Wu, Y., Yang, F., Rong, M. Z. (2020). Prediction of the electrical strength and boiling temperature of the substitutes for greenhouse gas SF_6 using neural network and random forest. *IEEE Access*, 8: 124204–124216.

[78] Wang, Y., Gao, Z. Y., Wang, B. S., Zhou, W. J., Yu, P., Luo, Y. B. (2019). Synthesis and dielectric properties of trifluoromethanesulfonyl fluoride: An alternative gas to SF_6. *Industrial & Engineering Chemistry Research*, 58: 21913–21920.

[79] Long, Y. X., Guo, L. P., Wang, Y., Chen, C., Chen, Y. H., Li, F., Zhou, W. J. (2020). Electron swarms parameters in CF_3SO_2F as an alternative gas to SF_6. *Industrial & Engineering Chemistry Research*, 59: 11355–11358.

[80] Hu, S. Z., Wang, Y., Zhou, W. J., Qiu, R., Luo, Y. B., Wang, B. S. (2020). Dielectric properties of CF_3SO_2F/N_2 and CF_3SO_2F/CO_2 mixtures as a substitute to SF_6. *Industrial & Engineering Chemistry Research*, 59: 15796–15804.

[81] Zhang, L., Peng, R. C., Huang, Y. J., Song, G. S., Wang, Y. (2022). Toxic study on the new eco-friendly insulating gas trifluoromethanesulfonyl fluoride: A substitute for SF_6. *Sustainability*, 14: 5239.

[82] Tian, S. S., Zhang, X. X., Cressault, Y., Hu, J. T., Wang, B., Xiao, S., Li, Y., Kabbaj, N. (2020). Research status of replacement gases for SF_6 in power industry. *AIP Advances*, 10: 050702.

[83] Takuma, T. (1999). Application of a gas mixture with c-C. In: Proceedings of the 11th International Symposium on High-Voltage Engineering (ISH 99). London, UK.

[84] Wada, J., Ueta, G., Okabe, S., Hikita, M. (2016). Dielectric properties of gas mixtures with per-fluorocarbon gas and gas with low liquefaction temperature. *IEEE Transactions on Dielectrics and Electrical Insulation*, 23: 838–847.

[85] Zhao, S., Jiao, J. T., Zhao, X. L., Zhang, H., Xiao, D. M., Yan, J. D. (2016). Synergistic effect of *c*-C_4F_8/N_2 gas mixtures in slightly non-uniform electric field under lightning impulse. In: Proceedings of the 2016 IEEE Electrical Insulation Conference (EIC). Montreal, Canada.

[86] Whitman, L. C. (1965). Impulse voltage tests on air and C_3F_8. *IEEE Transactions on Electrical Insulation*, EI-1: 44–48.

[87] Okubo, H., Yamada, T., Hatta, K., Hayakawa, N., Yuasa, S., Okabe, S. (2002). Partial discharge and breakdown mechanisms in ultra-dilute SF_6 and PFC gases mixed with N_2 gas. *Journal of Physics D: Applied Physics*, 35: 2760–2765.

[88] Xiao, S., Zhang, X. X., Han, Y. F., Dai, Q. W. (2016). AC breakdown characteristics of CF_3I/N_2 in a non-uniform electric field. *IEEE Transactions on Dielectrics and Electrical Insulation*, 23: 2649–2656.

[89] Zhang, X. X., Xiao, S., Han, Y. F., Dai, Q. W. (2015). Analysis of the feasibility of CF_3I/CO_2 used in C-GIS by partial discharge inception voltages in positive half cycle and breakdown voltages. *IEEE Transactions on Dielectrics and Electrical Insulation*, 22: 3234–3243.

[90] Toyota, H., Matsuoka, S., Hidaka, K. (2006). Measurement of sparkover voltage and time lag characteristics in $CF_3I–N_2$ and CF_3I–air gas mixtures by using steep-front square voltage. *Electrical Engineering in Japan*, 157: 1–7.

[91] Tu, Y. P., Luo, Y., Wang, C., Luo, S., Cheng, Y. C. (2015). Breakdown characteristics of CF_3I and CF_3I/N_2 gas mixtures in uniform field. In: Proceedings of the 2015 IEEE 11th International Conference on the Properties and Applications of Dielectric Materials (ICPADM). Sydney, Australia.

[92] Widger, P., Haddad, A., Griffiths, H. (2016). Breakdown performance of vacuum circuit breakers using alternative CF_3I-CO_2 insulation gas mixture. *IEEE Transactions on Dielectrics and Electrical Insulation*, 23: 14–21.

[93] Simka, P., Ranjan, N. (2015). Dielectric strength of C5 perfluoroketone. In: Proceedings of the 19th International Symposium on High Voltage Engineering, Pilzen, Czech.

[94] Saxegaard, M., Kristoffersen, M., Stoller, P., Seeger, M., Hyrenbach, M., Landsverk, H. (2015). Dielectric properties of gases suitable for secondary medium voltage switchgear. In: Proceedings of the 23rd International Conference on Electricity Distribution, Lyon, France.

[95] Tian, S. S., Zhang, X. X., Xiao, S., Deng, Z. T., Li, Y., Tang, J. (2019). Experimental research on insulation properties of $C_6F_{12}O/N_2$ and $C_6F_{12}O/CO_2$ gas mixtures. IET Generation. *Transmission & Distribution*, 13: 417–422.

[96] Kieffel, Y., Irwin, T., Ponchon, P., Owens, J. (2016). Green gas to replace SF_6 in electrical grids. *IEEE Power and Energy Magazine*, 14: 32–39.

[97] Nechmi, H. E., Beroual, A., Girodet, A., Vinson, P. (2016). Fluoronitriles/CO_2 gas mixture as promising substitute to SF_6 for insulation in high voltage applications. *IEEE Transactions on Dielectrics and Electrical Insulation*, 23: 2587–2593.

[98] Zhang, B. Y., Uzelac, N., Cao, Y. (2018). Fluoronitrile/CO_2 mixture as an eco-friendly alternative to SF_6 for medium voltage switchgears. *IEEE Transactions on Dielectrics and Electrical Insulation*, 25: 1340–1350.

[99] Li, Y., Zhang, X. X., Zhang, J., Fu, M. L., Zhuo, R., Luo, Y., Chen, D. C., Xiao, S. (2019). Experimental study on the partial discharge and AC breakdown properties of C_4F_7N/CO_2 mixture. *High Voltage*, 4: 12–17.

[100] Koch, M., Franck, C. M. (2015). High voltage insulation properties of HFO1234ze. *IEEE Transactions on Dielectrics and Electrical Insulation*, 22: 3260–3268.

[101] Hösl, A., Pachin, J., Egüz, E., Chachereau, A., Franck, C. M. (2020). Positive synergy of SF_6 and HFO1234ze(E). *IEEE Transactions on Dielectrics and Electrical Insulation*, 27: 322–324.

[102] Tu, Y. P., Cheng, Y., Wang, C., Ai, X., Zhou, F. W., Chen, G. (2018). Insulation characteristics of fluoronitriles/CO_2 gas mixture under DC electric field. *IEEE Transactions on Dielectrics and Electrical Insulation*, 25: 1324–1331.

[103] Wang, C., Cheng, Y., Tu, Y. P., Chen, G., Yuan, Z. K., Xiao, A., Owens, J., Zhang, A., Mi, N. (2018). Characteristics of C_3F_7CN/CO_2 as an alternative to SF_6 in HVDC-GIL systems. *IEEE Transactions on Dielectrics and Electrical Insulation*, 25: 1351–1356.

[104] Zheng, Y., Zhou, W. J., Li, H., Yan, X. L., Li, Z. B., Chen, W. J., Bian, K. (2019). Influence of conductor surface roughness on insulation performance of C_4F_7N/CO_2 mixed gas. *IEEE Transactions on Dielectrics and Electrical Insulation*, 26: 922–929.

[105] Xiao, S., Gao, B., Pang, X. P., Zhang, X. X., Li, Y., Tian, S. S., Tang, J., Luo, Y. (2021). The sensitivity of C_4F_7N to electric field and its influence to environment-friendly insulating gas mixture C_4F_7N/CO_2. *Journal of Physics D: Applied Physics*, 54: 055501.

[106] Ai, X., Tu, Y. P., Zhang, Y., Chen, G., Yuan, Z. K., Wang, C., Yan, X. L., Liu, W. (2020). The effect of electrode surface roughness on the breakdown characteristics of C_3F_7CN/CO_2 gas mixtures. *Inter-*

national Journal of Electrical Power & Energy Systems*, 118: 105751.

[107] Liu, J., Wang, F., Zhong, L. P., Chen, S., Sun, Q. Q., Nie, J., Tang, N., Li, L. (2023). Negative DC dielectric breakdown characteristics and synergistic effect of HFO-1336mzz(E) mixtures. *IEEE Transactions on Dielectrics and Electrical Insulation*, 30: 65–73.

[108] Tu, Y., Ai, X., Cheng, Y., Jin, H., Wang, C. (2018). DC breakdown characteristics of C_3F_7CN/N_2 gas mixtures. (in Chinese). *Transactions of China Electrotechnical Society*, 33: 5189–5195.

[109] Hu, S., Zhou, W., Zheng, Y. (2019). Power frequency breakdown experiments and synergistic effect analysis of C_4F_7N/CO_2 and C_4F_7N/N_2 mixtures. (in Chinese). *High Voltage Engineering (in Chinese)*, 45: 3562–3570.

[110] Zhao, S., Xiao, D. M., Zhang, H., Deng, Y. K. (2017). Discharge characteristics of CF_3I/N_2 mixtures under lightning impulse and alternating voltage. *IEEE Transactions on Dielectrics and Electrical Insulation*, 24: 2731–2737.

[111] Zhang, T. R., Zhou, W. J., Zheng, Y., Yu, J. H. (2019). Insulation properties of C_4F_7N/CO_2 mixtures under non-uniform electric field. *IEEE Transactions on Dielectrics and Electrical Insulation*, 26: 1747–1754.

[112] Xing, W. J., Zhang, G. Q., Li, K., Niu, W. H., Wang, X., Wang, Y. Y. (2011). Experimental study of partial discharge characteristics of c-C_4F_8/N_2 mixtures. (in Chinese). *Proceedings of the Chinese Society for Electrical Engineering*, 31: 119–124.

[113] Zhang, X., Zhou, J., Tang, J., Zhuo, R., Chen, Y. (2013). Experimental study of partial discharge insulating properties for CF_3I-CO_2 mixtures under needle-plate electrode. (in Chinese). *Transactions of China Electrotechnical Society*, 28: 36–42

[114] Toigo, C., Vu-Cong, T., Jacquier, F., Girodet, A. (2020). Partial discharge behavior of protrusion on high voltage conductor in GIS/GIL under high voltage direct current: Comparison of SF_6 and SF_6 alternative gases. *IEEE Transactions on Dielectrics and Electrical Insulation*, 27: 140–147.

[115] Li, Z. C., Ding, W. D., Gao, K. L., Liu, Y. S., Liu, W., Guo, Y. J. (2019). Surface flashover characteristics of epoxy insulator in C_4F_7N/CO_2 mixtures under lightening impulse voltage. (in Chinese). *High Voltage Engineering*, 45: 1071–1077.

[116] Chen, J. H., Sun, P., Li, J. S., Li, W. D., Li, Y., Deng, J. B., Ji, S. C., Zhang, G. J. (2022). Surface discharge pattern of C_4F_7N/CO_2 mixture under negative impulse voltages. *Applied Physics Letters*, 121: 171602.

[117] Chen, G., Tu, Y. P., Wu, S. C., Lin, C. J., Qin, S. C., Li, C. Y., He, J. L. (2020). Intrinsic hetero-polar surface charge phenomenon in environmental friendly C_3F_7CN/CO_2 gas mixture. *Journal of Physics D: Applied Physics*, 53: 18LT03.

[118] Zhang, R., Wang, J., Li, J., Ren, C. Y., Yan, P. (2017). Insulation characteristics of environmentally friendly mix gas c-C_4F_8/N_2 substituting SF_6. (in Chinese). *High Voltage Engineering*, 43: 414–419.

[119] Man, L., Deng, Y., Xiao, D. (2017). Insulating properties of c-C_4F_8/N_2 and c-C_4F_8/CO_2 mixtures. (in Chinese). *High Voltage Engineering*, 43: 788–794.

[120] Lin, L., Chen, Q. G., Wang, X. Y., Zhang, H., Feng, H. R., Zhang, C. (2018). AC breakdown characteristics of c-C_4F_8/N_2 gas mixtures in an extremely non-uniform electric field. *Energies*, 11: 3533.

[121] Zhang, Z. M., Ni, Z. R., Xiao, D. M., Wu, Y. Z. (2018). Insulation characteristics of triple mixtures of c-$C_4F_8/N_2/CO_2$ under lightning impulse voltage. *Plasma Science and Technology*, 20: 105405.

[122] Zhang, R., Wang, J., Yan, P. (2018). Insulation characteristics of c-C_4F_8/N_2 with less c-C_4F_8 applied to HVDC-GIL. (in Chinese). *High Voltage Engineering*, 44: 2672–2678.

[123] Man, L., Zhang, M., Pan, X., Lu, T., Yang, T., Sun, G. (2019). Surface flashover properties of c-C_4F_8/N_2 insulator. (in Chinese). *High Voltage Engineering*, 45: 1234–1240.

[124] Zhang, X. X., Xiao, S., Han, Y. F., Cressault, Y. (2016). Experimental studies on power frequency breakdown voltage of CF_3I/N_2 mixed gas under different electric fields. *Applied Physics Letters*, 108: 092901.

[125] Hu, S., Zhou, W., Zheng, Y., Zhang, T. R., Wang, L. Z., Li, Z. (2020). Influence of three buffer gases on dielectric strength of C_4F_7N mixtures. (in Chinese). *High Voltage Engineering*, 46: 224–232.

[126] Jiang, X., Jin, H. Y., Zhang, W. B. (2020). Lightning impulse insulation properties of eco-friendly C_4F_7N/CO_2 mixed gas under extremely non-uniform electric field. (in Chinese). *Proceedings of the Chinese Society for Electrical Engineering*. 40: 1030–1036).

[127] Li, Z. C., Ding, W. D., Liu, Y. S., Li, Y., Zheng, Z. B., Liu, W., Gao, K. L. (2019). Surface flashover characteristics of epoxy insulator in C_4F_7N/CO_2 mixtures in a uniform field under AC voltage. *IEEE Transactions on Dielectrics and Electrical Insulation*, 26: 1065–1072.

[128] Wang, X., Fu, X., Han, G., Lu, Y., Li, X., Gao, Q., Rong, M. (2017). Insulation performance of $C_5F_{10}O/CO_2$ gas mixture. (in Chinese). *High Voltage Engineering*, 43: 715–720.

[129] Guo, Z., Li, X. W., Li, B. X., Fu, M. L., Zhuo, R., Wang, D. B. (2019). Dielectric properties of C5-PFK mixtures as a possible SF_6 substitute for MV power equipment. *IEEE Transactions on Dielectrics and Electrical Insulation*, 26: 129–136.

[130] Zeng, F. P., Xie, B. Q., Su, D. Z., Li, C., Lei, Z. C., Ma, G. M., Dai, L. J., Li, L., Tang, J. (2022). Breakdown characteristics of eco-friendly gas $C_5F_{10}O/CO_2$ under switching impulse in nonuniform electric field. *IEEE Transactions on Dielectrics and Electrical Insulation*, 29: 866–873.

[131] Li, B. N., Fu, Y. J., Gao, Y. F., Niu, H., Li, M. R., Lang, J. Y., Li, S. T. (2022). Research on insulation properties of new environment-friendly gas $C_5F_{10}O/CO_2$. In: Proceedings of the 2022 IEEE International Conference on High Voltage Engineering and Applications (ICHVE). Chongqing, China.

[132] Lin, L., Chen, Q. G., Wang, X. Y., Zhang, H., Jia, Z. K., Zhang, C. (2020). Study on the decomposition mechanism of the HFO1234zeE/N_2 gas mixture. *IEEE Transactions on Plasma Science*, 48: 1130–1137.

[133] Ranjan, P., Chen, L., Alabani, A., Bahdad, F. O., Cotton, I., van der Zel, L. (2021). Anomalous first breakdown behavior for HFO1234ze(E). *IEEE Transactions on Dielectrics and Electrical Insulation*, 28: 1620–1627.

[134] Lesaint, O., Bonifaci, N., Merini, H., Maladen, R., Gentils, F. (2018). A study of breakdown properties of HFO gas under DC and impulse voltage. In Proceedings of the 2018 IEEE Conference on Electrical Insulation and Dielectric Phenomena (CEIDP). Cancun, Mexico.

[135] Zhong, L. L., Cressault, Y., Teulet, P. (2019). Evaluation of arc quenching ability for a gas by combining 1-D hydrokinetic modeling and boltzmann equation analysis. *IEEE Transactions on Plasma Science*, 47: 1835–1840.

[136] Cressault, Y., Teulet, P., Baumann, X., Vanhulle, G., Reichert, F., Petchanka, A., Kabbaj, N. (2019). State of art and challenges for the calculation of radiative and transport properties of thermal plasmas in HVCB. *Plasma Physics and Technology*, 6: 208–216.

[137] Cressault, Y., Connord, V., Hingana, H., Teulet, P., Gleizes, A. (2011). Transport properties of CF_3I thermal plasmas mixed with CO_2, air or N_2 as an alternative to SF_6 plasmas in high-voltage circuit breakers. *Journal of Physics D: Applied Physics*, 44: 495202.

[138] Zhong, L. L., Cressault, Y., Teulet, P. (2018). Thermophysical and radiation properties of high-temperature C_4F_8-CO_2 mixtures to replace SF_6 in high-voltage circuit breakers. *Physics of Plasmas*, 25: 033502.

[139] Zhong, L. L., Gu, Q., Wu, B. Y. (2021). Graphite production in two-temperature non-LTE plasmas of C_4F_7N and $C_5F_{10}O$ mixed with CO_2, N_2, and O_2 as eco-friendly SF_6 replacements: A numerical study. *Plasma Processes and Polymers*, 18: 2100036.

[140] Zhong, L. L., Wang, J. Y., Xu, J., Wang, X. H., Rong, M. Z. (2019). Effects of buffer gases on plasma properties and arc decaying characteristics of C_4F_7N–N_2 and C_4F_7N–CO_2 arc plasmas. *Plasma Chemistry and Plasma Processing*, 39: 1379–1396.

[141] Wu, Y., Wang, C. L., Sun, H., Murphy, A. B., Rong, M. Z., Yang, F., Chen, Z. X., Niu, C. P., Wang, X. H. (2018). Properties of C_4F_7N–CO_2 thermal plasmas: Thermodynamic properties, transport coefficients and emission coefficients. *Journal of Physics D: Applied Physics*, 51: 155206.

[142] Zhong, L. L., Rong, M. Z., Wang, X. H., Wu, J. H., Han, G. Q., Han, G. H., Lu, Y. H., Yang, A. J., Wu, Y. (2017). Compositions, thermodynamic properties, and transport coefficients of high-temperature $C_5F_{10}O$ mixed with CO_2 and O_2 as substitutes for SF_6 to reduce global warming potential. *AIP Advances*, 7: 075003.

[143] Wu, Y., Wang, C. L., Sun, H., Rong, M. Z., Murphy, A. B., Li, T. W., Zhong, J. Y., Chen, Z. X., Yang, F., Niu, C. P. (2017). Evaluation of SF_6-alternative gas C5-PFK based on arc extinguishing performance and electric strength. *Journal of Physics D: Applied Physics*, 50: 385202.

[144] Li, X. W., Guo, X. X., Murphy, A. B., Zhao, H., Wu, J., Guo, Z. (2017). Calculation of thermodynamic properties and transport coefficients of $C_5F_{10}O$-CO_2 thermal plasmas. *Journal of Applied Physics*, 122: 143302.

[145] Zhong, L. L., Wu, B. Y., Zheng, S. Z., Gu, Q. (2021). A database of electron-impact ionization cross sections of molecules composed of H, C, N, O, and F. *Physics of Plasmas*, 28: 083505.

[146] Zhong, L. L., Murphy, A. B., Wang, X. H., Rong, M. Z. (2020). Calculation of two-temperature plasma composition: II. Consideration of condensed phases. *Journal of Physics D: Applied Physics*, 53: 065203.

[147] Zhong, L. L., Wang, X. H., Rong, M. Z., Cressault, Y. (2016). Effects of copper vapour on thermophysical properties of CO_2-N_2 plasma. *The European Physical Journal D*, 70: 233.

[148] Liu, J., Zhang, Q., Yan, J. D., Zhong, J., Fang, M. C. (2016). Analysis of the characteristics of DC nozzle arcs in air and guidance for the search of SF_6 replacement gas. *Journal of Physics D: Applied Physics*, 49: 435201.

[149] Rong, M. Z., Zhong, L. L., Cressault, Y., Gleizes, A., Wang, X. H., Chen, F., Zheng, H. (2014). Thermophysical properties of SF_6–Cu mixtures at temperatures of 300–30, 000 K and pressures of 0.01–1.0 MPa: Part 1. Equilibrium compositions and thermodynamic properties considering condensed phases. *Journal of Physics D: Applied Physics*, 47: 495202.

[150] Teulet, P., Gonzalez, J. J., Mercado-Cabrera, A., Cressault, Y., Gleizes, A. (2009). One-dimensional hydro-kinetic modelling of the decaying arc in air–PA66–copper mixtures: II. Study of the interruption ability. *Journal of Physics D: Applied Physics*, 42: 185207.

[151] Salem, D., Hannachi, R., Cressault, Y., Teulet, P., Béji, L. (2017). Mean absorption coefficients of He/Ar/N_2/(C_{1-x-y}, Ni_x, Co_y) thermal plasmas for CNT synthesis. *Journal of Physics D: Applied Physics*, 50: 035203.

[152] Salem, D., Hannachi, R., Cressault, Y., Teulet, P., Béji, L. (2015). Radiative properties of argon–helium–nitrogen–carbon–cobalt–nickel plasmas used in CNT synthesis. *Journal of Physics D: Applied Physics*, 48: 065202.

[153] Cressault, Y., Bauchire, J. M., Hong, D., Rabat, H., Riquel, G., Sanchez, F., Gleizes, A. (2015). Radiation of long and high power arcs. *Journal of Physics D: Applied Physics*, 48: 415201.

[154] Cressault, Y. (2015). Basic knowledge on radiative and transport properties to begin in thermal plasmas modelling. *AIP Advances*, 5: 057112.

[155] Wang, X. H., Zhong, L. L., Rong, M. Z., Yang, A. J., Liu, D. X., Wu, Y., Miao, S. (2015). Dielectric breakdown properties of hot SF_6 gas contaminated by copper at temperatures of 300–3500 K. *Journal of Physics D: Applied Physics*, 48: 155205.

[156] Zhong, L. L., Yang, A. J., Wang, X. H., Liu, D. X., Wu, Y., Rong, M. Z. (2014). Dielectric breakdown properties of hot SF_6-CO_2 mixtures at temperatures of 300–3500 K and pressures of 0.01–1.0 MPa. *Physics of Plasmas*, 21: 053506.

[157] Hagelaar, G. M., Pitchford, L. C. (2005). Solving the Boltzmann equation to obtain electron transport coefficients and rate coefficients for fluid models. *Plasma Sources Science and Technology*, 14: 722–733.

[158] Wang, X. H., Zhong, L. L., Yan, J., Yang, A. J., Han, G. H., Han, G. Q., Wu, Y., Rong, M. Z. (2015). Investigation of dielectric properties of cold C_3F_8 mixtures and hot C_3F_8 gas as Substitutes for SF_6. *The European Physical Journal D*, 69: 240.

[159] Zhao, H., Li, X. W., Jia, S. L., Murphy, A. B. (2013). Dielectric breakdown properties of SF_6–N_2 mixtures at 0.01–1.6 MPa and 300–3000 K. *Journal of Applied Physics*, 113: 143301.

[160] Li, X. W., Zhao, H., Jia, S. L., Murphy, A. B. (2013). Study of the dielectric breakdown properties of hot SF_6–CF_4 mixtures at 0.01–1.6 MPa. *Journal of Applied Physics*, 114: 053302.

[161] Guo, Z., Liu, S. G., Pu, Y. J., Zhang, B. Y., Li, X. W., Tang, F., Lv, Q. S., Jia, S. L. (2019). Study of the arc interruption performance of CO_2 gas in high-voltage circuit breaker. *IEEE Transactions on Plasma Science*, 47: 2742–2751.

[162] Pu, Y. J., Tang, F., Zhang, B. Y., Zhou, R., Li, X. W. (2020). Study of the arc interruption performance of SF_6 alternative gases in load switch. In: Proceedings of the 2020 IEEE International Conference on High Voltage Engineering and Application (ICHVE). Beijing, China.

[163] Yokomizu, Y., Suzuki, M., Matsumura, T. (2006). Thermodynamic, transport and radiation properties of high-temperature CF_3I and transient conductance of residual arc sustained in axial CF_3I flow. *IEEJ Transactions on Electrical and Electronic Engineering*, 1: 268–275.

[164] Zhong, L. L., Gu, Q., Zheng, S. Z. (2019). An improved method for fast evaluating arc quenching performance of a gas based on 1D arc decaying model. *Physics of Plasmas*, 26: 103507.

[165] Guo, Z., Tang, F., Lv, Q., Li, X., Zhang, B., Jia, S., Huang, R. (2019). Experimental investigation on the arc characteristics and arc quenching capabilities of $C_5F_{10}O$-CO_2 mixtures. *Plasma Physics and Technology*, 6: 231–234.

[166] Chen, L., Zhang, B. Y., Yang, T., Deng, Y. K., Li, X. W., Murphy, A. B. (2020). Thermal decomposition characteristics and kinetic analysis of C_4F_7N/CO_2 gas mixture. *Journal of Physics D: Applied Physics*, 53: 055502.

[167] Li, Y., Zhang, X. X., Zhang, J., Xie, C., Shao, X. J., Wang, Z. L., Chen, D. C., Xiao, S. (2020). Study on the thermal decomposition characteristics of C_4F_7N–CO_2 mixture as eco-friendly gas-insulating medium. *High Voltage*, 5: 46–52.

[168] Xiao, S., Li, Y., Zhang, X. X., Tian, S. S., Deng, Z. T., Tang, J. (2017). Effects of micro-water on decomposition of the environment-friendly insulating medium $C_5F_{10}O$. *AIP Advances*, 7: 065017.

[169] Zhang, X. X., Li, Y., Shao, X. J., Xie, C., Chen, D. C., Tian, S. S., Xiao, S., Tang, J. (2019). Influence of oxygen on the thermal decomposition properties of C_4F_7N–N_2–O_2 as an eco-friendly gas insulating medium. *ACS Omega*, 4: 18616–18626.

[170] Zhang, B. Y., Li, C. W., Xiong, J. Y., Zhang, Z. Y., Li, X. W., Deng, Y. K. (2019). Decomposition characteristics of C_4F_7N/CO_2 mixture under AC discharge breakdown. *AIP Advances*, 9: 115212.

[171] Li, Y., Zhang, X. X., Xiao, S., Chen, Q., Tang, J., Chen, D. C., Wang, D. B. (2018). Decomposition properties of C_4F_7N/N_2 gas mixture: An environmentally friendly gas to replace SF_6. *Industrial & Engineering Chemistry Research*, 57: 5173–5182.

[172] Tang, N., Chen, L., Zhang, B. Y., Li, X. W. (2020). Experimental and theoretical exploration of C_4F_7N gas decomposition under partial discharge. In: Proceedings of the 2020 IEEE International Conference on High Voltage Engineering and Application (ICHVE). Beijing, China.

[173] Zhang, X. X., Li, Y., Xiao, S., Tang, J., Tian, S. S., Deng, Z. T. (2017). Decomposition mechanism of $C_5F_{10}O$: An environmentally friendly insulation medium. *Environmental Science & Technology*, 51: 10127–10136.

[174] Zhang, Y., Zhang, X. X., Li, Y., Li, Y. L., Chen, Q., Zhang, G. Z., Xiao, S., Tang, J. (2019). AC breakdown and decomposition characteristics of environmental friendly gas $C_5F_{10}O$/air and $C_5F_{10}O/N_2$.

IEEE Access, 7: 73954–73960.
[175] Li, Y. L., Zhang, X. X., Li, Y., Wei, Z., Ye, F. C., Xiao, S., Zhang, X. X., Wang, Y. (2021). Effect of oxygen on power frequency breakdown characteristics and decomposition properties of C5-PFK /CO_2 gas mixture. *IEEE Transactions on Dielectrics and Electrical Insulation*, 28: 373–380.
[176] Li, Y. L., Zhang, X. X., Wang, Y., Li, Y., Zhang, Y., Wei, Z., Xiao, S. (2019). Experimental study on the effect of O_2 on the discharge decomposition products of C5-PFK/N_2 mixtures. *Journal of Materials Science: Materials in Electronics*, 30: 19353–19361.
[177] Wang, X. N., Ma, J., Liu, D. X., Ma, Q., Yuan, H., Yang, A. J., Rong, M. Z., Wang, X. H. (2021). Detection and analysis of spark discharge products of $C_5F_{10}O$ by electron attachment mass spectrometry. *Journal of Physics D: Applied Physics*, 54: 045201.
[178] Wang, X. N., Wang, X. H., Yuan, H., Yang, A. J., Liu, D. X., Gao, Q. Q., Rong, M. Z. (2022). Study on the insulation performance and decomposition characteristics of $C_5F_{10}O/CO_2$ gas mixture. *Plasma Chemistry and Plasma Processing*, 42: 957–971.
[179] Zhang, Y., Zhang, X. X., Li, Y., Li, Y. L., Chen, Q., Zhang, G. Z., Xiao, S., Tang, J. (2019). Effect of oxygen on power frequency breakdown voltage and decomposition characteristics of the $C_5F_{10}O$ /N_2/O_2 gas mixture. *RSC Advances*, 9: 18963–18970.
[180] Li, Y., Zhang, X. X., Chen, Q., Zhang, J., Li, Y. L., Xiao, S., Tang, J. (2019). Influence of oxygen on dielectric and decomposition properties of C_4F_7N-N_2-O_2 mixture. *IEEE Transactions on Dielectrics and Electrical Insulation*, 26: 1279–1286.
[181] Li, Y., Zhang, X. X., Ye, F. C., Chen, D. C., Tian, S. S., Cui, Z. L. (2020). Influence regularity of O_2 on dielectric and decomposition properties of C_4F_7N–CO_2–O_2 gas mixture for medium-voltage equipment. *High Voltage*, 5: 256–263.
[182] Ye, F. C., Zhang, X. X., Li, Y., Yao, Y. H., Xiao, S., Zhang, X. X., Xie, C., Shao, X. J., Sun, X. (2021). Effect of O_2 on AC partial discharge and decomposition behavior of $C_4F_7N/CO_2/O_2$ gas mixture. *IEEE Transactions on Dielectrics and Electrical Insulation*, 28: 1440–1448.
[183] Fu, Y. W., Yang, A. J., Wang, X. H., Rong, M. Z. (2019). Theoretical study of the decomposition mechanism of C_4F_7N. *Journal of Physics D: Applied Physics*, 52: 245203.
[184] Zhang, X. X., Li, Y., Xiao, S., Tian, S. S., Deng, Z. T., Tang, J. (2017). Theoretical study of the decomposition mechanism of environmentally friendly insulating medium C_3F_7CN in the presence of H_2O in a discharge. *Journal of Physics D: Applied Physics*, 50: 325201.
[185] Fu, Y. W., Wang, X. H., Li, X., Yang, A. J., Han, G. H., Lu, Y. H., Wu, Y., Rong, M. Z. (2016). Theoretical study of the decomposition pathways and products of C5- perfluorinated ketone (C5 PFK). *AIP Advances*, 6: 085305.
[186] Zhang, X. X., Li, Y., Chen, D. C., Xiao, S., Tian, S. S., Tang, J., Zhuo, R. (2017). Reactive molecular dynamics study of the decomposition mechanism of the environmentally friendly insulating medium C_3F_7CN. *RSC Advances*, 7: 50663–50671.
[187] Liu, Y., Hu, J. Y., Hou, H., Wang, B. S. (2020). ReaxFF reactive force field development and application for molecular dynamics simulations of heptafluoroisobutyronitrile thermal decomposition. *Chemical Physics Letters*, 751: 137554.
[188] Li, Y., Zhang, X. X., Tian, S. S., Xiao, S., Li, Y. L., Chen, D. C. (2019). Insight into the decomposition mechanism of $C_6F_{12}O$-CO_2 gas mixture. *Chemical Engineering Journal*, 360: 929–940.
[189] Zhang, X. X., Li, Y., Tian, S. S., Xiao, S., Chen, D. C., Tang, J., Zhuo, R. (2018). Decomposition mechanism of the C5-PFK/CO_2 gas mixture as an alternative gas for SF_6. *Chemical Engineering Journal*, 336: 38–46..
[190] Li, Y., Zhang, X. X., Xiao, S., Chen, Q., Wang, D. B. (2018). Decomposition characteristics of $C_5F_{10}O$/air mixture as substitutes for SF_6 to reduce global warming. *Journal of Fluorine Chemistry*, 208: 65–72.
[191] Gao, Q. Q., Wang, X. H., Adamiak, K., Qi, X. C., Yang, A. J., Liu, D. X., Niu, C. P., Zhang, J. W. (2022). Negative corona discharge mechanism in C_4F_7N–CO_2 and C_4F_7N–N_2 mixtures. *AIP Advances*, 12: 095101.
[192] Atanasova-Höhlein, I. (2021). Compatibility of materials with insulating liquids—Why and how to test. *IEEE Electrical Insulation Magazine*, 37: 31–35.
[193] Gao, W. Q., Cao, Y., Wang, Y. F., Price, C., Ronzello, J., Uzelac, N., Laso, A., Tefferi, M., Darko, K. (2022). Materials compatibility study of C_4F_7N/CO_2 gas mixture for medium-voltage switchgear. *IEEE Transactions on Dielectrics and Electrical Insulation*, 29: 270–278.
[194] Xiong, J. Y., Zhang, B. Y., Zhang, Z. Y., Deng, Y. K., Li, X. W. (2020). The adsorption properties of environmentally friendly insulation gas C_4F_7N on Zn (0001) and ZnO (101¯0) surfaces: A first-principles study. *Applied Surface Science*, 509: 144854.
[195] Li, Y., Zhang, X. X., Xiao, S., Chen, D. C., Chen, Q., Wang, D. B. (2018). Theoretical evaluation of the interaction between C5-PFK molecule and Cu (1 1 1). *Journal of Fluorine Chemistry*, 208: 48–54.
[196] Li, Y., Zhang, X. X., Xiao, S., Chen, D. C., Liu, C., Shi, Y. (2018). Insights into the interaction between C_4F_7N decomposition products and Cu (1 1 1), Ag (1 1 1) surface. *Journal of Fluorine Chemistry*, 213: 24–30.
[197] Li, Y., Zhang, X. X., Tian, S. S., Xiao, S., Chen, Q., Chen, D. C., Cui, Z. L., Tang, J. (2018). Insight into the compatibility between $C_6F_{12}O$ and metal materials: Experiment and theory. *IEEE Access*, 6: 58154–58160.
[198] Li, Y., Zhang, X. X., Xiao, S., Zhang, J., Chen, D. C., Cui, Z. L. (2019). Insight into the compatibility between C_4F_7N and silver: Experiment and theory. *Journal of Physics and Chemistry of Solids*, 126: 105–111.
[199] Xiao, S., Li, Y., Zhang, X. X., Zhang, J., Zhang, Y., Chen, D. C., Tang, J. (2019). Theoretical study on the interaction of heptafluoroiso-butyronitrile decomposition products with Al (1 1 1). *Molecular Physics*, 117: 218–227.
[200] Li, Y., Zhang, X. X., Chen, Q., Zhang, J., Chen, D. C., Cui, Z. L., Xiao, S., Tang, J. (2019). Study on the thermal interaction mechanism between C_4F_7N-N_2 and copper, aluminum. *Corrosion Science*, 153: 32–46.
[201] Li, Y. L., Zhang, Y., Li, Y., Tang, F., Lv, Q. S., Zhang, J., Xiao, S., Tang, J., Zhang, X. X. (2019). Experimental study on compatibility of eco-friendly insulating medium $C_5F_{10}O/CO_2$ gas mixture with copper and aluminum. *IEEE Access*, 7: 83994–84002.
[202] Zhang, X. X., Wang, Y. F., Li, Y., Li, Y. L., Ye, F. C., Tian, S. S., Chen, D. C., Xiao, S., Tang, J. (2019). Thermal compatibility properties of $C_6F_{12}O$-air gas mixture with metal materials. *AIP Advances*, 9: 125024.
[203] Li, Y. L., Zhang, X. X., Xia, Y. L., Li, Y., Wei, Z., Wang, Y., Xiao, S. (2020). Study on the compatibility of eco-friendly insulating gas $C_5F_{10}O/N_2$ and $C_5F_{10}O$/air with copper materials in gas-insulated switchgears. *Applied Sciences*, 11: 197.
[204] Kessler, F., Sarfert-Gast, W., Kuhlmann, L., Ise, M., Heinemann, F. W. (2020). Compatibility of a gaseous dielectric with Al, Ag, and Cu and gas-phase synthesis of a new *N*-acylamidine copper complex. *European Journal of Inorganic Chemistry*, 2020: 1989–1994.
[205] Zhang, X. X., Li, Y., Chen, D. C., Xiao, S., Tian, S. S., Tang, J., Wang, D. B. (2018). Dissociative adsorption of environment-friendly insulating medium C_3F_7CN on Cu(111) and Al(111) surface: A theoretical evaluation. *Applied Surface Science*, 434: 549–560.
[206] Li, Y., Zhang, X. X., Chen, D. C., Li, Y. L., Zhang, J., Cui, Z. L., Xiao, S., Tang, J. (2019). Theoretical study on the interaction between C5-PFK and Al (1 1 1), Ag (1 1 1): A comparative study. *Applied Surface Science*, 464: 586–596.
[207] Yuan, R. J., Li, H., Zhou, W. J., Zheng, Z. Y., Yu, J. H. (2020). Study of compatibility between epoxy resin and C_4F_7N/CO_2 based on thermal ageing. *IEEE Access*, 8: 119544–119553.
[208] Wang, C., Cao, R. J., Tu, Y. P., Ai, X., Zhang, Y., Xu, Y. S. (2021). Characteristics of C_4F_7N/epoxy resin insulation system affected by

long-term electro-thermal accelerated aging. *IEEE Transactions on Dielectrics and Electrical Insulation*, 28: 1973–1979.

[209] Wang, C., Ai, X., Zhang, Y., Tu, Y. P., Liu, W., Yan, X. L., Bai, C. Y. (2020). Decomposition characteristics and marker products of C_3F_7CN/EP insulation system with long-term surface discharge. *Engineering Failure Analysis*, 116: 104719.

[210] Li, Y., Zhang, X. X., Li, Y. L., Chen, D. C., Cui, Z. L., Liu, W., Tang, J. (2020). Interaction mechanism between the C_4F_7N–CO_2 gas mixture and the EPDM seal ring. *ACS Omega*, 5: 5911–5920.

[211] Zhang, X. X., Wu, P., Cheng, L., Liang, S. C. (2021). Compatibility and interaction mechanism between EPDM rubber and a SF_6 alternative gas—$C_4F_7N/CO_2/O_2$. *ACS Omega*, 6: 13293–13299.

[212] Zhang, Y., Liu, J., Huang D., Wang, Y., Zeng, L. (2020). Effect of insulating and enviromental gas C_4F_7N and CO_2 on aging resistance of EPDM and NBR. (in Chinese). *China Rubber Industry*, 67: 0177–0180.

[213] Xiao, S., Chen, J. Y., Wu, P., Yao, Q., Li, L., Pang, X. P., Zhang, S. L., Zhang, X. X., Li, Y. (2023). Research on the adsorption of environmentally friendly insulating gas C_4F_7N decomposed components on the surface of γ-Al_2O_3. *High Voltage*, 8: 274–282.

[214] Xiao, S., Chen, D. C., Tang, J., Li, Y. (2020). Adsorption behavior of γ-Al_2O_3 toward heptafluoroisobutyronitrile and its decompositions: Theoretical and experimental insights. *IEEE Access*, 8: 36741–36748.

[215] Zhao, M., Han D., Zhou L., Zhang, G. (2020). Adsorption characteristics of activated aluminaand molecular sieves for C_3F_7CN/CO_2 and its decomposition by-products of overheating fault. (in Chinese). *Transactions of China Electrotechnical Society*, 35: 88–96.

[216] Hou, H., Yan X., Yu X., Liu, W., Liu, Z., Wang, B. (2020). Theoretical investigation on the adsorption of C_4F_7N/CO_2 dielectric gas and decomposition products in zeolite. (in Chinese). *High Voltage Engineering*, 45: 1040–1047.

[217] Tian, S. S., Yuan, Z. A., Zhang, X. X., Wang, Y. X., Luo, W. F., Liu, Y. (2022). Adsorption properties of environmentally friendly insulating medium C_4F_7N and its common decomposition products in NaA, NaZSM-5, and NaX molecular sieves. *High Voltage*, 2022: 1–11.

[218] Material Toxicity Summary Sheet, 3M™ Novec™ 4710 Insulating Gas; 3M Company: St. Paul, MN, USA, 2019.

[219] Material Toxicity Summary Sheet, 3M™ Novec™ 5110 Insulating Gas; 3M Company: St. Paul, MN, USA, 2019.

[220] Li, Y., Zhang, X. X., Zhang, J., Xiao, S., Xie, B. J., Chen, D. C., Gao, Y. D., Tang, J. (2019). Assessment on the toxicity and application risk of C_4F_7N: A new SF_6 alternative gas. *Journal of Hazardous Materials*, 368: 653–660.

[221] Zhang, X. X., Ye, F. C., Li, Y., Tian, S. S., Xie, B. J., Gao, Y. D., Xiao, S. (2020). Acute toxicity and health effect of perfluoroisobutyronitrile on mice: A promising substitute gas-insulating medium to SF_6. *Journal of Environmental Science and Health, Part A*, 55: 1646–1658.

[222] Carles, A., Schlernitzauer, A., Vignes, M., Cros, G., Magous, R., Maurice, T., Oiry, C. (2022). Heptafluoroisobutyronitrile (C_4F_7N), a gas used for insulating and arc quenching in electrical switchgear, is neurotoxic in the mouse brain. *Toxicology*, 480: 153319.

[223] Meyer, F., Huguenot, P., Kieffel, Y., Maksoud, L., Huet, I., Berteloot, M., Walter, T., Owens, J. G., Bonk, J., Schlernitzauer, R., Van San, A., Magous, R. (2020). Application of fluoronitrile/CO_2/O_2 mixtures in high voltage products to lower the environmental footprint. *Water and Energy International*, 63r: 75.

[224] Ye, F. C., Zhang, X. X., Li, Y., Wan, Q. Q., Bauchire, J. M., Hong, D. P., Xiao, S., Tang, J. (2022). Arc decomposition behavior of C_4F_7N/Air gas mixture and biosafety evaluation of its by-products. *High Voltage*, 7: 856–865.

[225] Preve, C., Maladen, R., Piccoz, D. (2019). Alternative gases to SF_6 as breaking medium for switching performance: Measurement of the concentrations of by-products and assessment of the acute toxicity. In: Proceedings of the 21st International Symposium on High Voltage Engineering (ISH), Budapest, Hungary.

[226] Kristoffersen, M., Endre, T., Saxegaard, M., Hyrenbach, M., Wang, P. A., Harmsen, D., van Rijn, T., Vosse, R. (2017). Ring main units with eco-efficient gas mixtures: Field experience. *CIRED - Open Access Proceedings Journal*, 2017: 412–415.

[227] Tian, S. S., Zhang, X. X., Wang, Y., Rao, X. J., Ye, F. C., Li, Y., Xiao, S. (2019). Partial discharge characteristics of $C_6F_{12}O/CO_2$ mixed gas at power frequency AC voltage. *AIP Advances*, 9: 095057.

[228] Chen, R., Li, W., Dong, E. Y., Wang, Y. X., Zhang, L. F., Yuan, F., Zhang, J. F. (2022). Analysis of arc characteristics of C_4F_7N/CO_2 mixed gas ring main unit. *IEEE Transactions on Plasma Science*, 50: 1948–1956.

[229] Preve, C., Maladen, R., Trichon, F., Piccoz, D. (2019). Innovative SF_6 free switch with shunt vacuum interruption technology. In: Proceedings of the 25th International Conference on Electricity Distribution, Madrid, Spain.

[230] Preve, C., Maladen, R., Trichon, F., Piccoz, D., Penelon, T., Richaud, M., Galas, S., Cros, G. (2018). HFO1234zeE in medium voltage switchgear as safe alternative to SF6. https://e-cigre.org/publication/SESSION2018_D1-105.

[231] Inversin., M., Tsamo, D. S., Luescher, R., Moulle, G., Kieffel, Y., (2020). Alternative to SF6: an on-site 145 kV GIS pilot project from a TSO perspective. https://e-cigre.org/publication/SESSION2020_B3-115.

[232] Gautschi, D., Ficheux, A., Walter, M., Vuachet, J. (2016). Application of a fluoronitrile gas in GIS and GIL as an environmental friendly alternative to SF6. https://e-cigre.org/publication/B3-106_2016.

[233] Claessens, M. (2018). Physical aspects of arc interruption in CO_2/O_2/fluoroketones gas mixtures. https://e-cigre.org/publication/SESSION2018_A3-305.

[234] Kuschel, M., Kunde, K., Katschinski, U. (2019). Technically advanced and SF6-free 145 kV blue GIS. *Transformers Magazine*, 6: 110–115.

[235] Kuschel, M., Albert, A., Ehrlich, F., Nesheim, N., Pohlink, K., Rank, T., Skar, J. (2020). First 145 kV/40 kA gas-insulated switchgear with climate-neutral insulating gas & vacuum interrupter as an alternative to SF6-design, manufacturing, qualification & operational experience. Available at: https://e-cigre.org/publication/SESSION2020_B3-107.

[236] Kim, K., Heo, S., Choi B., Kuschel, M., Ehrlich, F., Rank, T., Pohlink, K. First 170 kV/50 kA GIS with clean air and vacuum interrupter technology as a climate-neutral alternative to SF6 Available at: https://e-cigre.org/publication/SESSION2020_A3-301.

[237] Zhang, Y., Zhang, X. X., Liu, C., Li, Y., Cui, Z. L., Fu, M. L. (2019). Ultraviolet spectral analysis and quantitative detection of heptafluoroisobutyronitrile (C_4F_7N) in a C_4F_7N–carbon dioxide (CO_2) gas mixture. *Applied Spectroscopy*, 73: 917–926.

[238] Kramer, A., Over, D., Stoller, P., Paul, T. A. (2017). Fiber-coupled LED gas sensor and its application to online monitoring of ecoefficient dielectric insulation gases in high-voltage circuit breakers. *Applied Optics*, 56: 4505.

[239] Li, Y. L., Li, Y., Wei, Z., Zhang, X. X., Chen, W. J., Xiao, S., Tang, J., Bauchire, J. M., Hong, D. P. (2022). Quantification of C5-PFK gas mixture based on ultraviolet differential optical absorption spectroscopy (UV-DOAS). *IEEE Transactions on Dielectrics and Electrical Insulation*, 29: 394–402.

[240] Zhang, Y., Zhang, X. X., Liu, C., Li, Y., Cheng, H. T., Xiao, H. (2019). Research on C_4F_7N gas mixture detection based on infrared spectroscopy. *Sensors and Actuators A: Physical*, 294: 126–132.

[241] Zhang, X. X., Zhang, Y., Huang, Y., Li, Y., Cheng, H. T., Xiao, S. (2020). Detection of decomposition products of C_4F_7N-CO_2 gas mixture based on infrared spectroscopy. *Vibrational Spectroscopy*, 110: 103114.

[242] Porus, M., Paul, T. A., Kramer, A. (2017). Application of a multiparameter sensor system for monitoring dielectric insulation of gas mixtures. *IEEE Transactions on Dielectrics and Electrical Insulation*, 24: 847–851.

[243] Wu, P., Li, Y., Xiao, S., Chen, J. Y., Tang, J., Chen, D. C., Zhang, X. X. (2022). SnO_2 nanoparticles based highly sensitive gas sensor for detection of C_4F_7N: A new eco-friendly gas insulating medium. *Journal of Hazardous Materials*, 422: 126882.

[244] Wu, P., Li, Y., Xiao, S., Chen, D. C., Chen, J. Y., Tang, J., Zhang, X. X. (2022). Room-temperature detection of perfluoroisobutyronitrile with $SnO_2/Ti_3C_2T_x$ gas sensors. *ACS Applied Materials & Interfaces*, 14: 48200–48211.

[245] 3M News Center. (2022) 3M to Exit PFAS Manufacturing by the End of 2025 Available at: https://news.3m.com/2022-12-20-3M-to-Exit-PFAS-Manufacturing-by-the-End-of-2025.